NAS-CR-72148·

N 67 16563

(ACCESSION NUMBER) (THRU)

(PAGES) (CODE)

NASA CR - 72148

(NASA CR OR TMX OR AD NUMBER) (CATEGORY)

STUDY OF ASBESTOS FOR

ELECTROCHEMICAL CELLS

FIRST SUMMARY REPORT

DECEMBER 28, 1966

Prepared for

National Aeronautics and Space Administration

Lewis Research Center

Under Contract NAS 3-8522

TRW EQUIPMENT LABORATORIES

CLEVELAND. OHIO

NAS-CR-72148

First Summary Report

STUDY OF ASBESTOS FOR

ELECTROCHEMICAL CELLS

Prepared by::

J. W. Vogt

for

National Aeronautics and Space Administration

December 28, 1966

Contract No. NAS 3-8522

Technical Management:

NASA - Lewis Research Center
Rankine and Electrochemistry Branch
Daniel G. Soltis

Materials Research and Development Department
TRW Equipment Laboratories
23555 Euclid Avenue
Cleveland, Ohio 44117

FOREWORD

This report is the Task I Summary Report for Contract NAS 3-8522: "Study of Asbestos for Electrochemical Cells". This project has the goal of characterizing the Johns Manville Fuel Cell Grade Asbestos presently used in electrochemical cells, and to examine other asbestoses and different inorganic fibrous materials in search for a superior material for cell separator application. Task I of this project was the study of the Johns Manville asbestos; Task II will be the study of the other materials. The Task I effort, which is summarized in this report, represents approximately one half of the program effort and correspondingly represents about a six-month effort of the total one-year program.

The NASA technical director for this contract is Daniel G. Soltis. The author wishes to acknowledge him for the several helpful discussions held during the course of this work.

Prepared by _____

J. W. Vogt
Principal Engineer

Approved by _____

D. P. Laverty
Section Manager

Approved by _____

G. J. Guarnieri,
Manager, Materials
Research and Development

TABLE OF CONTENTS

INTRODUCTION

This program is concerned with the testing of "Fuel Cell Asbestos" and of selected alternate materials for use as the electrolyte matrix in a fuel cell. Although the Arizona chrysotile which constitutes Fuel Cell Asbestos is almost ideal in some respects, there are other properties which limit the cell performance. Each of the tests specified relates to a physical or chemical property of the material which pertains to its function as a matrix material. Many of the tests are intended to reveal the magnitude of property variations rather than absolute values.

It is anticipated that the tests comprising this program will contribute to an explanation for the failures of the material in service, aid in formulating a preliminary testing and materials selection program, and contribute guidance to the search for improved materials.

The first part of the program comprises the tests of chrysotile fuel cell asbestos. In the second part, similar tests are to be applied to modified asbestos and to selected inorganic synthetic fibrous materials. Where justified, recommendations will be made for improvement of the materials available for matrix application.

MANUFACTURE OF FUEL CELL ASBESTOS

The paper and millboard manufactured by Johns Manville for fuel cell use is Arizona chrysotile. Not possessing any natural deposits of this material, Johns Manville must buy it from an independent sole source. Johns Manville is, therefore, unable to control to its satisfaction the quality and uniformity of the raw-material.

The raw chrysotile is processed at the paper mill at Tilton, New Hampshire. This is a super-clean plant, planned and built for the manufacture of Quinterra chrysotile paper and millboard for critical application as electrical insulator material. Johns Manville personnel are satisfied that this plant is uniquely capable of producing asbestos sheet of the quality required for fuel cell use. They are also convinced, however, that the asbestos, being a natural fiber not subject to adequate control, is too variable in properties to be a component in a successful commercial fuel cell. There is, therefore, no economic motivation for their engagement in developmental work to improve the fuel cell asbestos. It is being produced by strictly conventional techniques as an accommodation to the customers engaged in fuel cell development. Currently, the customers are subjecting the material to 100% inspection and must reject about one-half of the material as unsuitable.

The plant site at Tilton was selected because a lake there provided an abundant supply of water of acceptable purity. However, in recent years, population development in the region has increased the contamination level in the water. Sanitary waste materials have increased the water fertility for growth of algae, and it has become necessary to add chemical suppressants to the water used in processing asbestos. The water pollutants and the additives will appear in the final paper, and although they have not been detrimental to the performance of Quinterra electrical insulation, they may very well introduce new problems in fuel cell development.

The raw chrysotile is crushed and ground until the desired fiber length and separation is attained. It is then dispersed in pure water to form a slurry of about 0.5% solids. A drum with wire mesh periphery, rotating partially submerged in the slurry, picks up a thin layer of fibers. Water inside the drum is continuously pumped out to maintain a hydraulic pressure differential by virtue of which the inward flow of slurry occurs.

In the manufacture of paper, the layer of fibers is transferred to a traveling wool felt belt, and by a repetition of similar transfers, a layer of desired thickness is accumulated on the belt. It is then passed through pressing rolls, the asbestos layer is lifted from the wool felt, passed through a drier and finally rolled on a mandrel.

The manufacture of millboard is somewhat different. The primary layer of fibers is transferred to a wool belt and immediately transferred to a rotating drum, on which a sufficient thickness is allowed to accumulate. The layer is then cut and stripped from the roll, placed flat on a metal tray, and dried in an oven.

The paper is compacted by pressing rolls; the millboard is not.

The manufacturing operations tend to establish an orientation of fibers tangent to the rotating drum surface. This orientation is revealed in the tensile tests to be described later. Another effect is that wool fibers, standing erect from the felt surface, will cause small holes in the asbestos mat. These holes may appear in the final paper or millboard.

It is usually true that the paper or millboard obtained early in the production run is different from the rest. One contributory factor is that the water, containing extreme fines, is recycled. The concentration of fines gradually attains a constant level when their incorporation in the mat is balanced by the rate of supply in new fibers. Consequently, the concentration of very fine, short fibers in the finished sheet is low at the start of a run and increases gradually to a level which persists to the end of the run.

EXPERIMENTAL PROGRAM

The chrysotile sheet stock to be tested was selected from the warehouse stocks on hand at the Johns Manville Tilton plant. One 25-sheet lot was cut from the leading end of a roll of 20-mil paper; another similar lot, from the trailing end. One 25-sheet lot of 60-mil millboard was cut from the start of a production run; another lot from the end of the same run. These four lots were given special care in handling and were specially packaged to prevent damage during shipping.

Upon receipt at TRW, the four lots were identified numerically as follows:

> 1000 series - 60 mil millboard-start of run
> 2000 series - 60 mil millboard-end of run
> 3000 series - 20 mil paper - start of run
> 4000 series - 20 mil paper - end of run

From each of the lots, 5 sheets were selected at random and identified numerically, for example, 1100, 1200, 1300, 1400, 1500. Each sheet was then cut into sections and identified for testing (1101, 1102, etc.). In each case, a one-inch margin was trimmed from each edge of the sheet in order to remove material that may have suffered physical damage. These trimmed edges were then used for some of the tests of properties that are independent of fiber packing.

The chrysotile paper and millboard were tested to yield, insofar as possible, quantitative values for the physical and chemical properties which pertain to their performance as an electrolyte matrix material. These tests ranged from tests of the basic material and fiber properties to studies of the behavior of the saturated mat in an electrolytic conductor.

Specifically, the tests were the following:

Asbestos Fiber Properties:

    Chemical Analysis
    Photographic and electron micrographic examination
    Surface area measurements

Dry Mat Properties:

    Tensile test
    Permeability to gas
    Density
    Thickness variation
    Pore size distribution

Wet Mat Properties (Wet with KOH electrolyte)

    Electrolyte absorption and retention
    Electrolytic conductivity of saturated mat
    Permeability to gas

Chemical Degradation Tests

Electrochemical Degradation Tests

TESTS AND RESULTS

A. Asbestos Properties

Chemical analysis. - Two oven-dried chrysotile specimens were analyzed by standard wet methods. The specimens were digested for several hours with hydrochloric acid and filtered. The residue was ignited, weighed, and heated with HF to volatilize the silica. After weighing, the non-volatile residue was dissolved in HCl and added to the filtrate containing the acid solubles. The iron group ions were double-precipitated with NH_4OH-NH_4Cl and ignited. From the filtrate, calcium was precipitated as oxalate and ignited, and magnesium was precipitated as the ammonium phosphate and ignited. No attempt was made to resolve the R_2O_3 group into the usual constituents Fe, Al, etc.

Following are the results of this analysis:

	Specimen	
	No. 1	No. 2
SiO_2	41. 86%	42. 14%
MgO	42. 78	42. 80
CaO	2. 19	1. 70
Fe_2O_3	0. 85	0. 87

The remainder (about 12%) is water which can be driven off by high temperature treatment.

Photographic and electronmicrographic examination. - A piece of black vinyl "Electricians" tape was pressed lightly against the surface of a piece of the 60-mil millboard, and the fibers adhering to the surface were photographed at 10X (Figure 1). There are visible many very fine fiber bundles, several evident stalks of unresolved fibers, and several wads of very fine fibers.

The electron micrographic specimen was prepared by impressing the plastic replica material against an asbestos sheet. Fibers of the asbestos were retained by the plastic. The replica sheet was shadowed with chromium on carbon at about 20° angle. The photographs (Figure 2) made at 20, 000X reveal that fibers of 0. 01 mil diameter are bundles of many smaller fibers. These photographs do not permit an estimate of ultimate fiber diameter, but they do suggest the enormous porosity potential of the natural material.
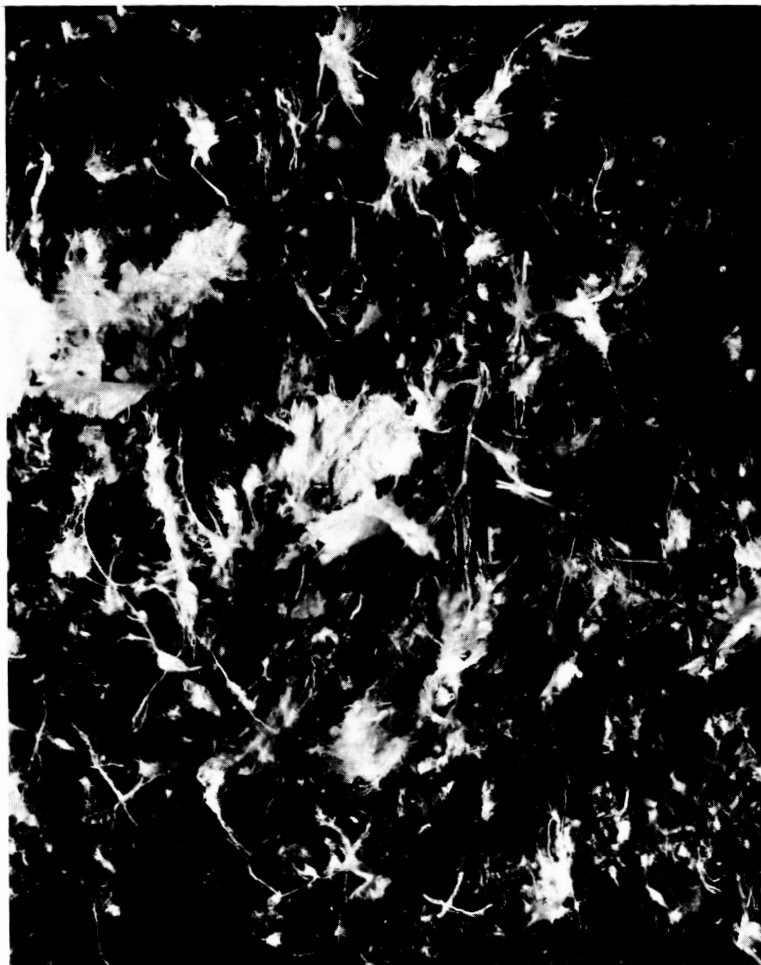
Figure 1.   Chrysotile asbestos fibers; 10x

4314A

Figure 2.   Electronmicrograph of chrysotile fibers;   20,000x

8

Surface area measurements. – These measurements were made with the Perkin Elmer Sorptometer, Model 212B. The instrument was standardized against materials obtained from American Instrument Co. and standardized by the Bone Char Research Project, Inc. (originated by The National Bureau of Standards). Following are the average surface areas reported by the Bone Char Project and the values obtained by TRW Inc.

	Bone Char Project	TRW
Reference Absorbent No. 2	10.3 m^2/gm	10.38 m^2/gm
Reference Absorbent No. 6	69.2	75.6
Reference Absorbent No. 8	560	515

The TRW values compare favorably with the span of values upon which the Bone Char Project averages are based.

One specimen of each of the asbestos stocks yielded the following values.

Specimen Number	Surface Area
1200	50.7 m^2/gm
2400	48.5
3100	55.5
4100	48.3

These values are in very close agreement, and they indicate that the property is not significantly dependent on the variables in the processes of converting suspended chrysotile pulp into paper and millboard.

B. Dry Mat Properties

Tensile tests. – Tensile tests were performed on an Instron Tensile Tester. The specimens were die-cut rectangles (2 x 3 inches) mounted to provide a gage length of 1 inch. Cross-head speed was 0.50 inch per minute.

In one set of tests, one specimen was taken from each of twenty test sheets. There were five sheets each of the material designated as 1000, 2000, 3000, and 4000 series. The tensile specimens were cut at random angles with respect to the processing direction of the material. The results are summarized in Table 1 and the load-elongation curves are presented, super-

Table 1 - Tensile Tests

Specimen No.	Loading Angle	Load (lbs.)*
1100	45°	21.675
1200	0	18.975
1300	30	19.675
1400	50	16.575
1500	20	19.80
2100	60°	10.05
2200	30	9.475
2300	45	16.95
2400	90	10.75
2500	0	10.75
3100	0	6.625
3200	0	6.325
3300	45	6.650
3400	45	7.25
3500	90	8.90
4100	0	6.05
4200	45	6.725
4300	45	7.35
4400	90	6.95
4500	0	6.175

* This is maximum load for specimens with a cross-sectional area of 2 inches times the thickness of the asbestos mat (0.055" for the 1000 and 2000 series specimens and 0.020" for the 3000 and 4000 series).

imposed, in Figures 3, 4, 5, and 6. For the 20-mil paper, the values of load at failure and the curve shapes are reasonably similar. For the 60-mil millboard, however, the values of load-at-failure differ widely, and the elongation curves reveal different modes of failure. Some specimens failed after moderate extension while others stretched much more before failure. These tests did not reveal a clear relationship between mode of failure and angle of loading relative to processing direction.

A second set of tests was conducted to clarify the influence of direction of loading on the shape of the elongation curves. Two presumably similar sheets of the same stock (2000 series) were cut into specimens. One sheet (2701) furnished nine specimens, all with the loading direction parallel to the processing direction. The other sheet furnished six specimens parallel (2702A) and four specimens tranverse (2702B) to the processing direction. The elongation curves for these tests are presented in superimposed groups in Figures 7, 8, and 9. (Two curves are omitted; they were unsatisfactory because the specimen slipped in the grips during test.)

The curves reveal that loading in the transverse direction causes about 0.07 inch extension before abrupt failure. Loading in the parallel direction causes about 0.15 inch extension at a much lower stress level. This probably reflects a preferential orientation of the asbestos fibers parallel to the processing direction. Parallel loading apparently involves considerable slippage between the parallel oriented fibers. In transverse loading, less slippage of the fibers occurs. It is interesting that in tearing of the 20-mil paper, which is roll-compressed, there is not a similar dependence of failure mode on angle of loading.

Density and porosity. – True volume of the specimens was measured with the Beckmann Air-Comparison Pycnometer. The technique employed by this instrument intrudes air into all the open porosity of the specimen and, thereby, determines the density of the asbestos fibers. The instrument was standardized against the two steel balls furnished by the manufacturer, and the zero error was determined immediately prior to measurement of each specimen.

One large specimen of each sample lot of asbestos was measured, and the data are recorded below.

A   1100   45°
B   1200   0°
C   1300   30°
D   1400   50°
E   1500   20°
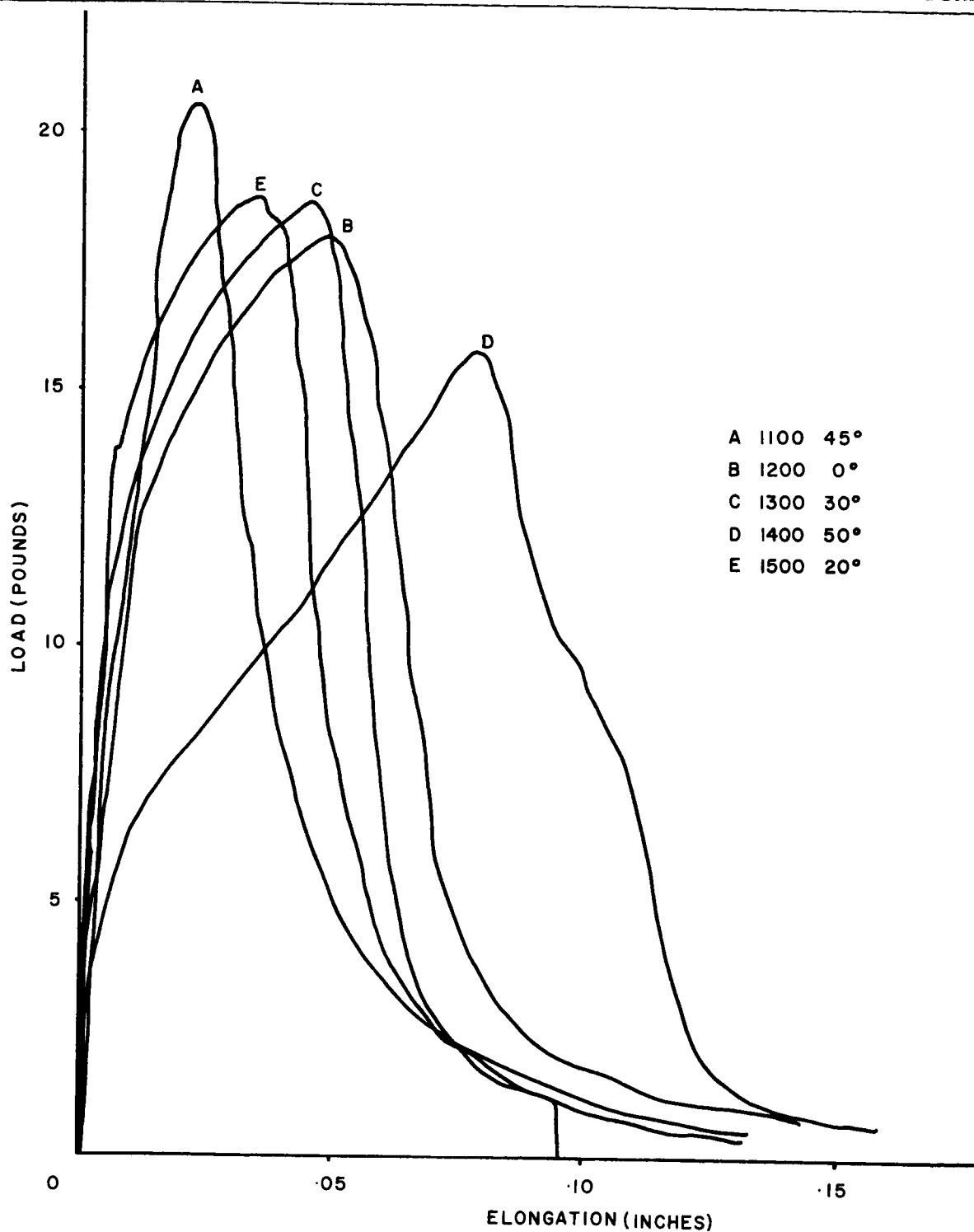
Figure 3.   Tensile test results of 60-mil asbestos board (1000 series) taken at various angles with respect to the processing direction.
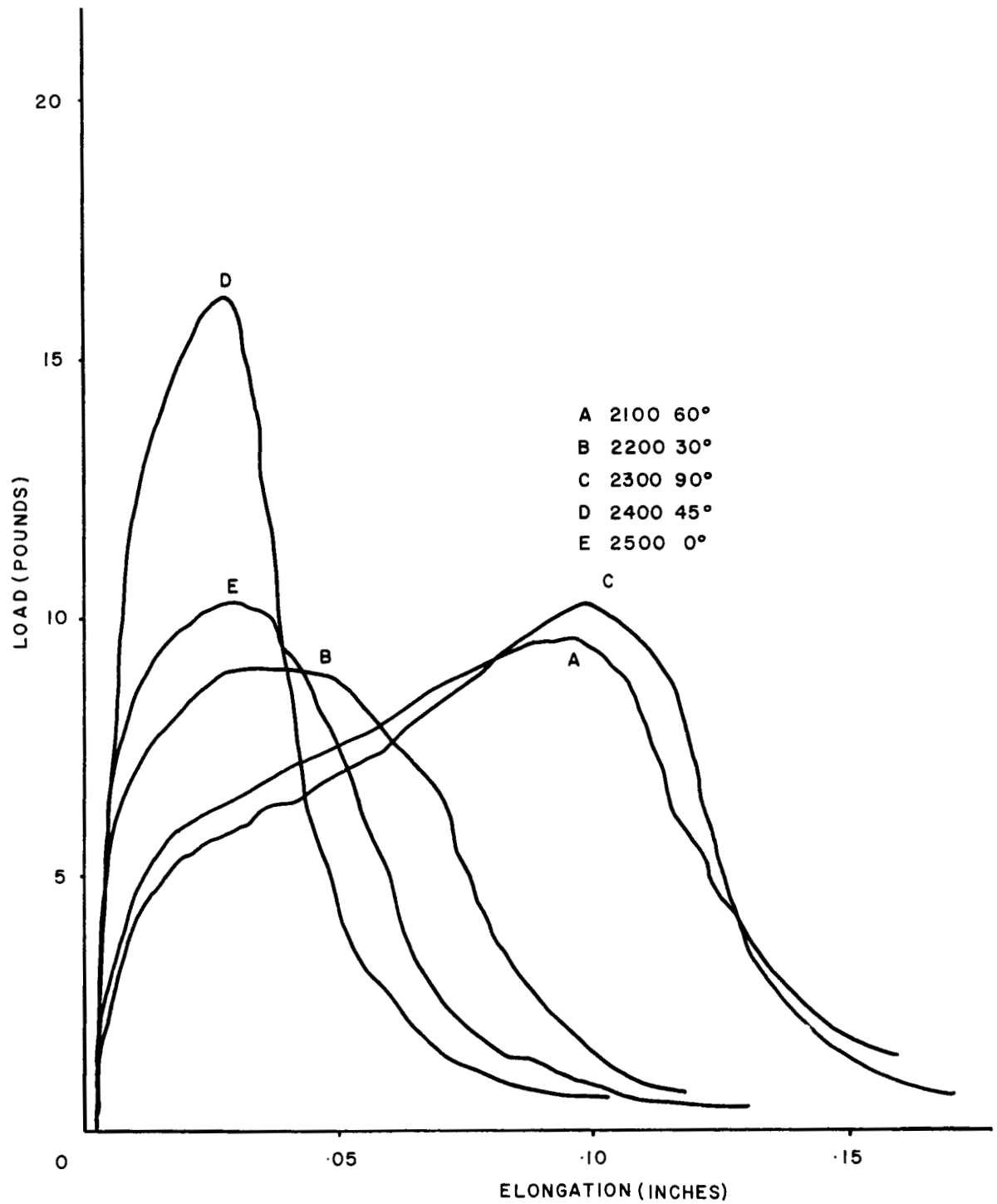
Figure 4. Tensile test results of 60-mil asbestos board (2000 series) taken at various angles with respect to the processing direction.

13

L302A
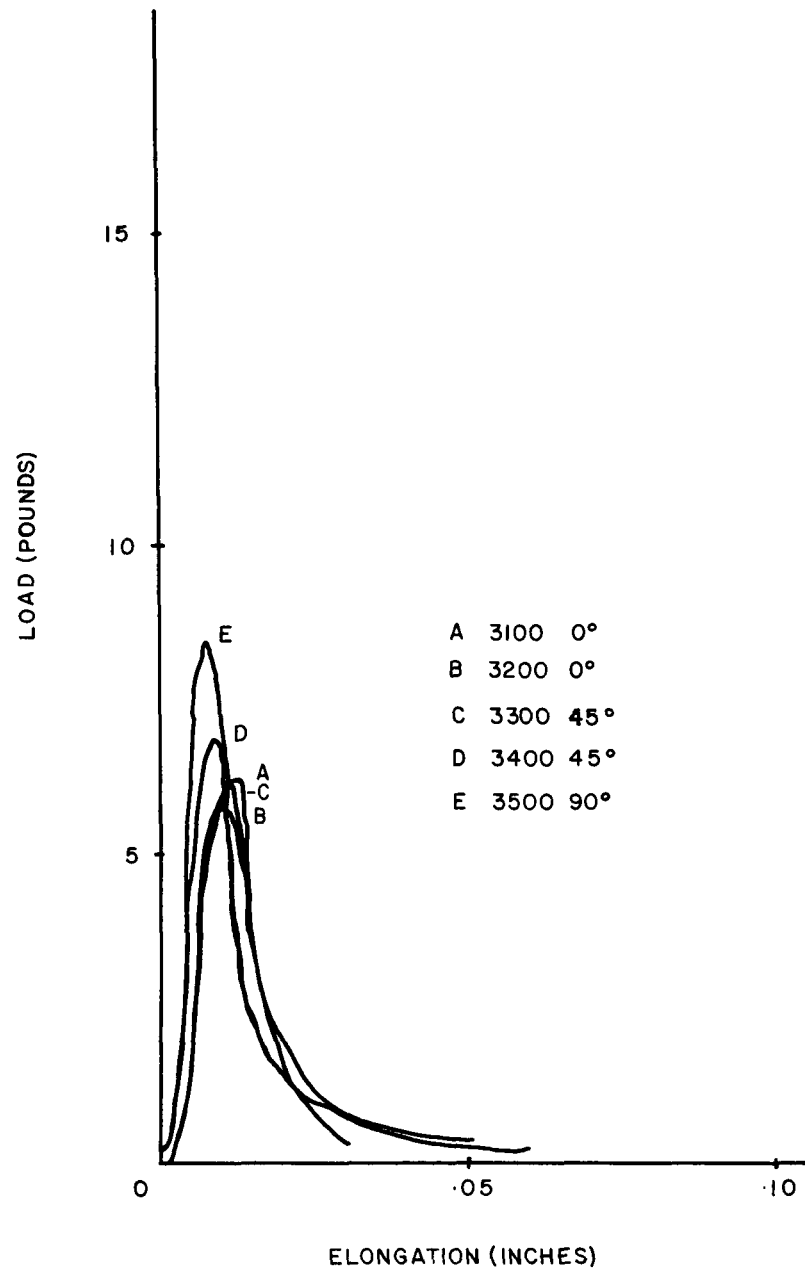
Figure 5. Tensile test results of 20-mil asbestos paper (3000 series) taken at various angles from the processing direction.

14

43034
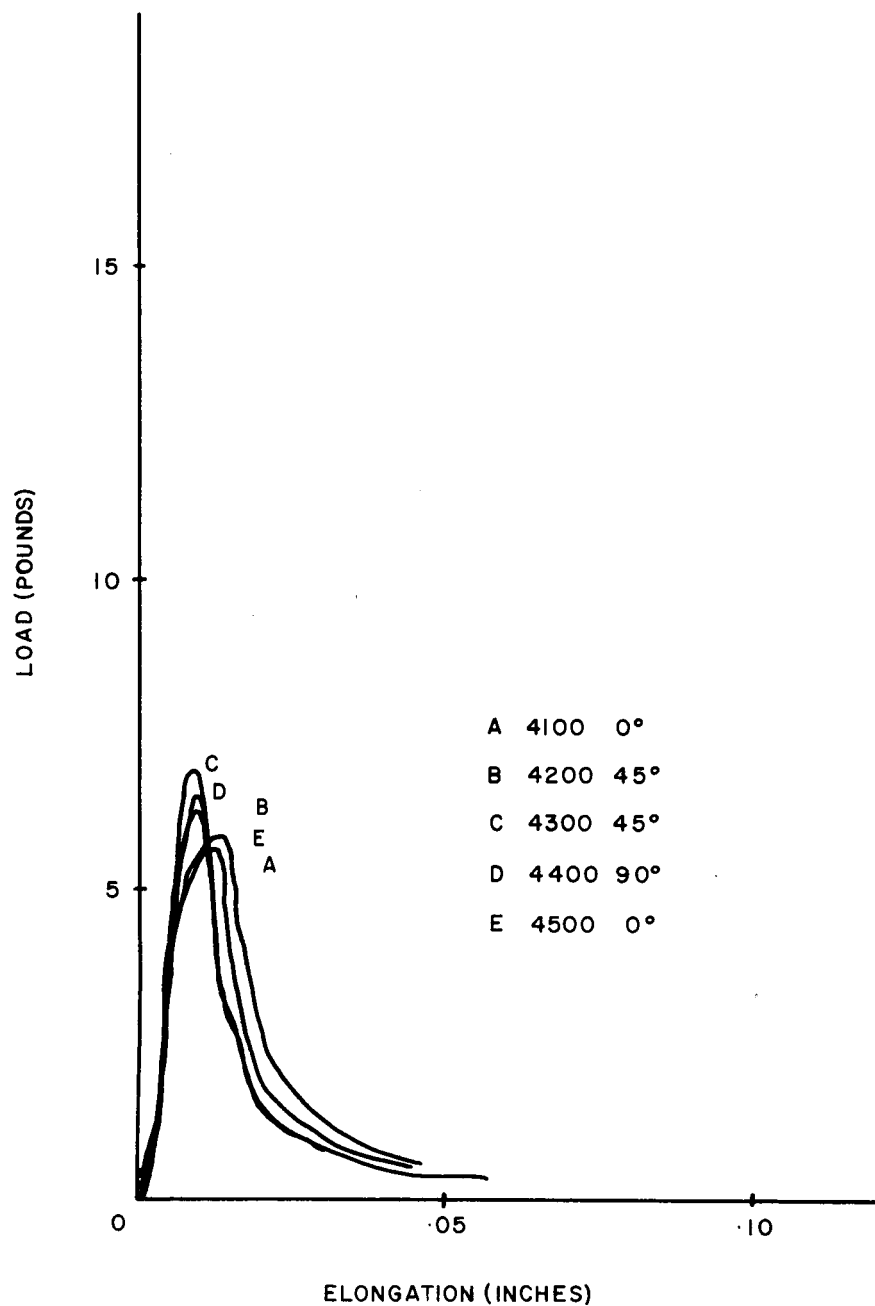
Figure 6. Tensile test results of 20-mil asbestos paper (4000 series) taken at various angles from the processing direction.
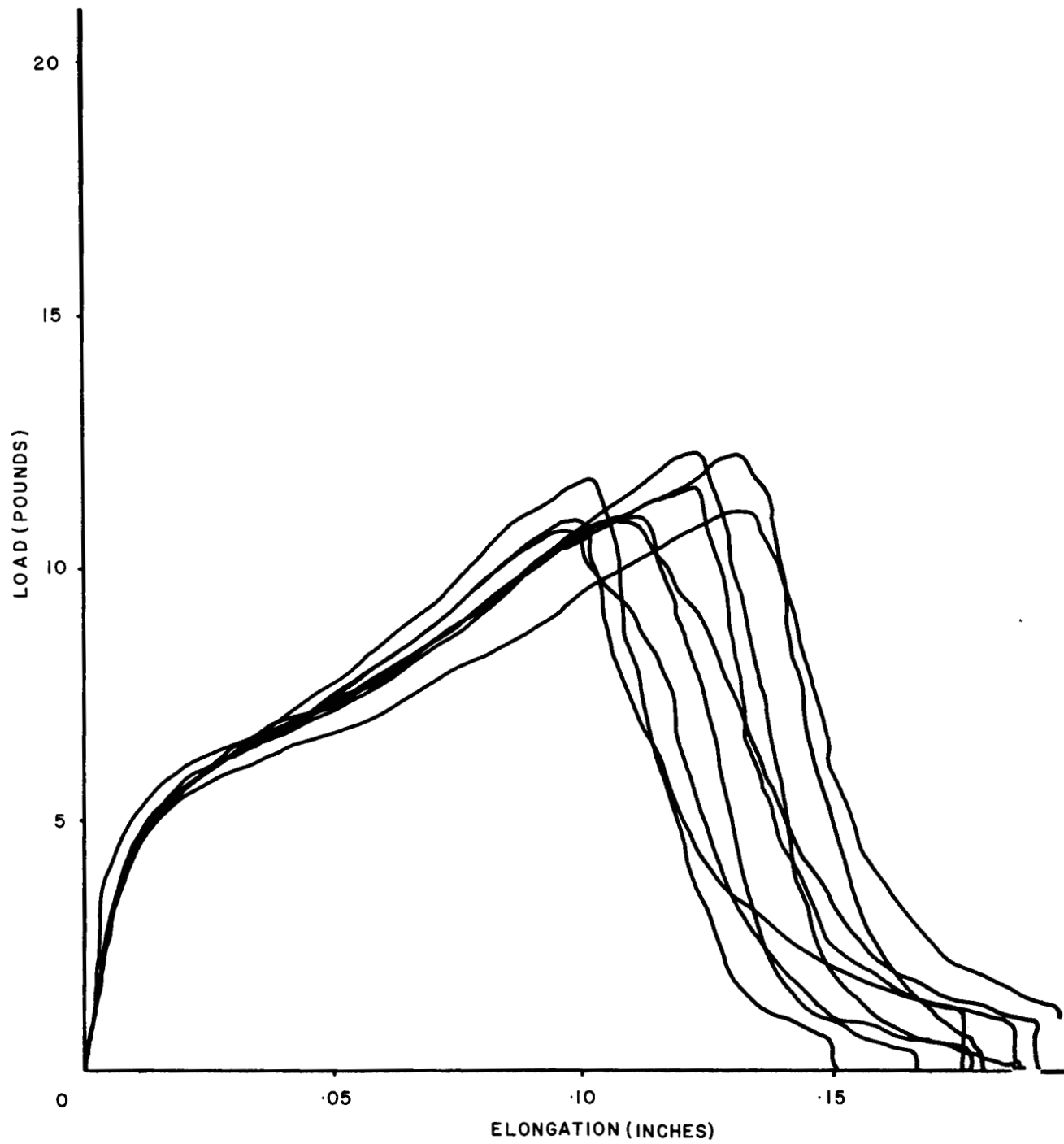
Figure 7.   Tensile test results of nine parallel samples from a sheet
of 60-mil asbestos board (specimen 2701) all taken parallel
to the processing direction.

4310A
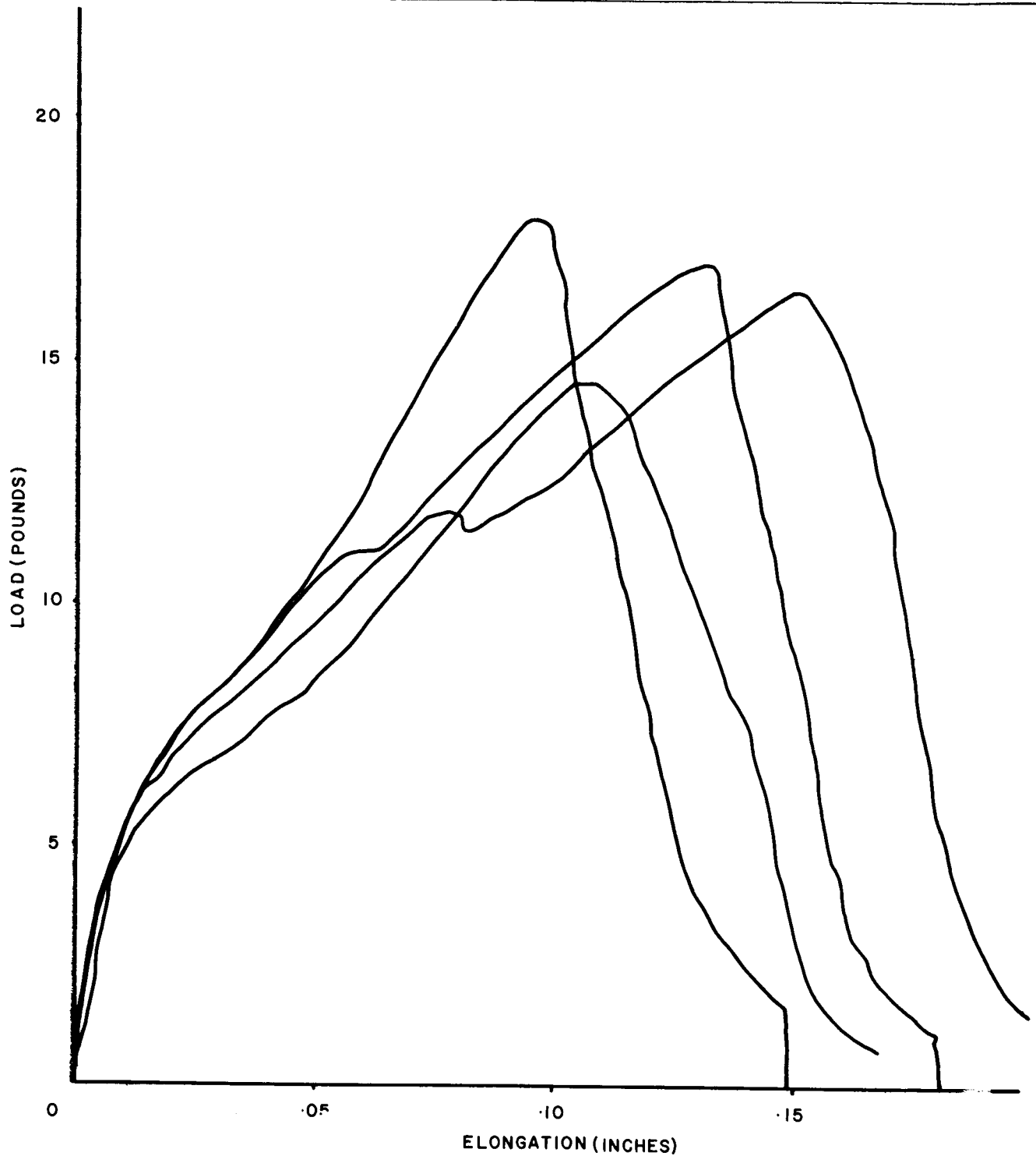
Figure 8.   Tensile test results of four similarly-oriented samples from a sheet of 60-mil board (specimen 2702) all taken parallel to the processing direction.
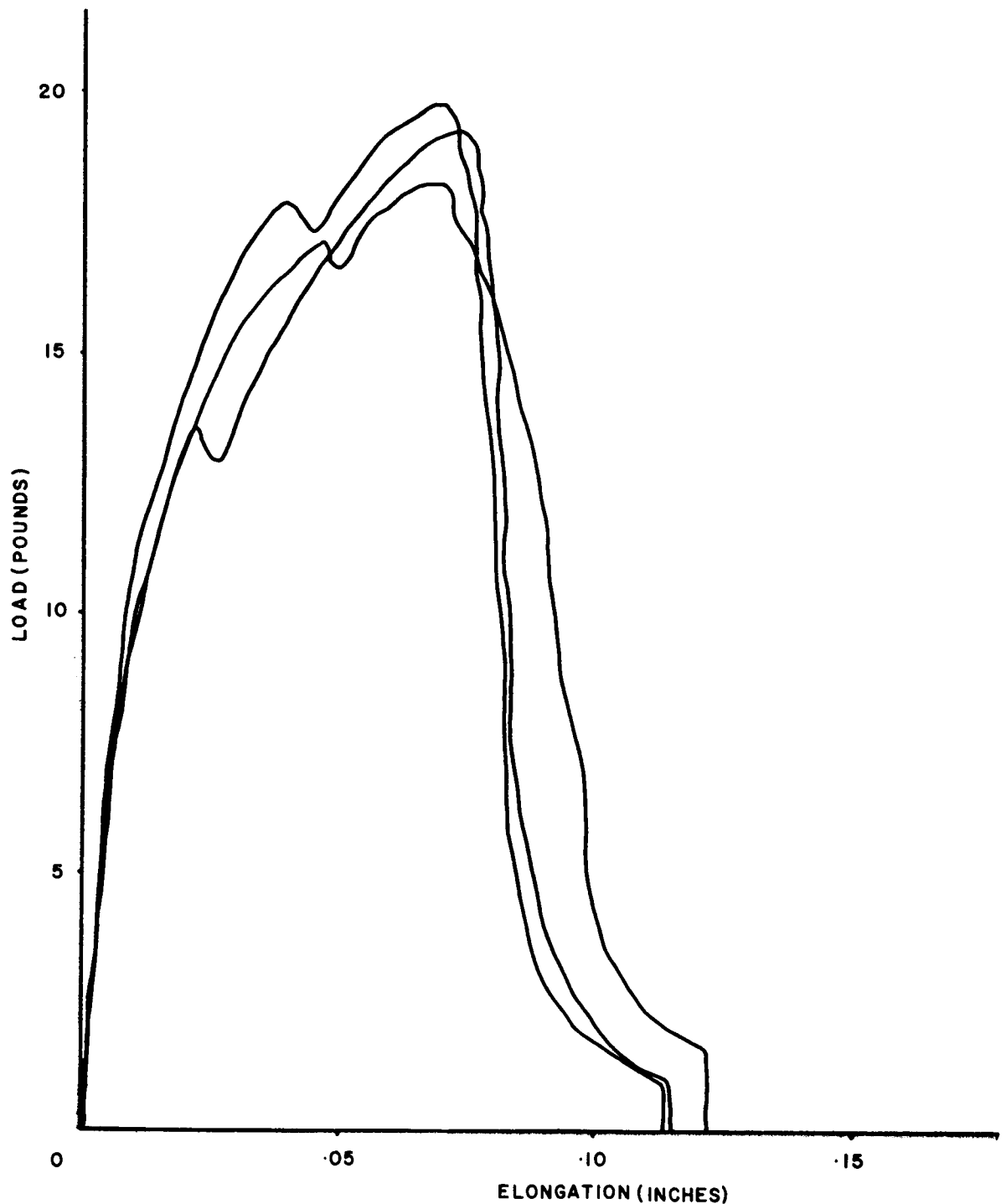
Figure 9. Tensile test results of three samples taken from the same sheet of material as referred to in Figure 8 (specimen 2702) but these specimens were taken transverse to the processing direction of the asbestos board.

18

Specimen	Weight, gm	Volume (Corrected), cc	Density g/cc
1000	25.2270	9.26	2.724
2000	20.4995	7.55	2.715
3000	15.0466	5.51	2.731
4000	14.6849	5.32	2.760

Thus, the asbestos used to make the millboard (1000 and 2000 series) appear to be slightly less dense than that used in the paper (3000 and 4000 series).

For estimation of the percentages of theoretical density of the dry sheet material, several sheets of each specimen series were weighed, and the densities were calculated from the geometric volume. The data tabulated below reveal that the paper is slightly more dense than the millboard as a result of the rolling operation experienced by the paper in its manufacture.

	60-mil millboard		20-mil paper	
		Specimen Series		
	1000	2000	3000	4000
Average sheet thickness (in.)	0.0550	0.0480	0.0205	0.0196
Number of sheets weighed	3	3	5	5
Total weight (g)	214.0	181.3	145.8	141.1
Geometric volume (cm^3)	253	221	157.2	150.4
Density (g/cm^3)	0.847	0.820	0.928	0.939
Density (air pyc.)g/cm^3	2.724	2.715	2.731	2.760
% Density	31.1	30.2	34.0	34.1

These data show that the 20-mil paper is about 66% porous in the dry mat state whereas the 60-mil material is about 70% porous. In the electrolyte-saturated state, however, the mats expand considerably, so the porosity of the asbestos mats in the cell environment will be considerably higher than that measured in the dry state.

Gas permeability. – Permeability of the dry specimens was measured as an incidental part of testing the wet specimens for gas permeability. This test, and the apparatus, is described in more detail later.

Generally, air flow through the dry specimen, as indicated by a bubbler, began when the pressure gradient was less than 1 inch of water. In several instances, the flow rate was measured at increasing pressures until the bubbler became unreliable as a rate indicator. These data are plotted in Figure 10.

The porosity of the specimen can be described satisfactorily, within the effective range of use of the bubbler in terms of the slope of the rate-versus-pressure curve. The slopes of these curves for the dry specimens are given in Table 2.

Note that where measurements were made over a small pressure range on specimens 2100 and 2500, the calculated flow rate/pressure ratios were fairly constant. On the contrary, the ratios for the 4200, 4300, and 4400 series increase markedly with slight increase in pressure. Thus, the millboard gas permeability can be described by a single ratio value at low pressure, whereas the ratio for the 20-mil paper cannot.

Thickness variation. – Measurements of thickness were made with a Federal Dial gage instrument, equipped with a 0.5-inch diameter foot and dead-weighted for a pressure of 5 lbs./sq. inch. This pressure seemed adequate to prevent arching of the specimen. In making a measurement, the gage foot was lowered gently to the specimen surface to prevent crushing the mat by impact. Each specimen piece was measured at four different locations chosen at random. The results are presented graphically in Figure 11.

It is evident that the paper is more uniform than the millboard. This probably reflects the fact that the paper is compressed whereas the millboard is not. Also, the actual thickness of the paper is quite near the nominal value, while the millboard, which is nominally 1/16" thick (or 0.0625 inch), is actually about 0.055 inch.

One may reasonably assume that the data for the paper are representative, but no such interpretation may be accepted for the millboard. The millboard thickness depends mainly on the quantity of fiber accumulated on the drum surface for each sheet. These observations may justify the postulation that the measured thickness of asbestos is not pertinent to fuel cell application, but rather the weight per unit area may be a preferable index of the quantity of fiber being provided between the electrodes.
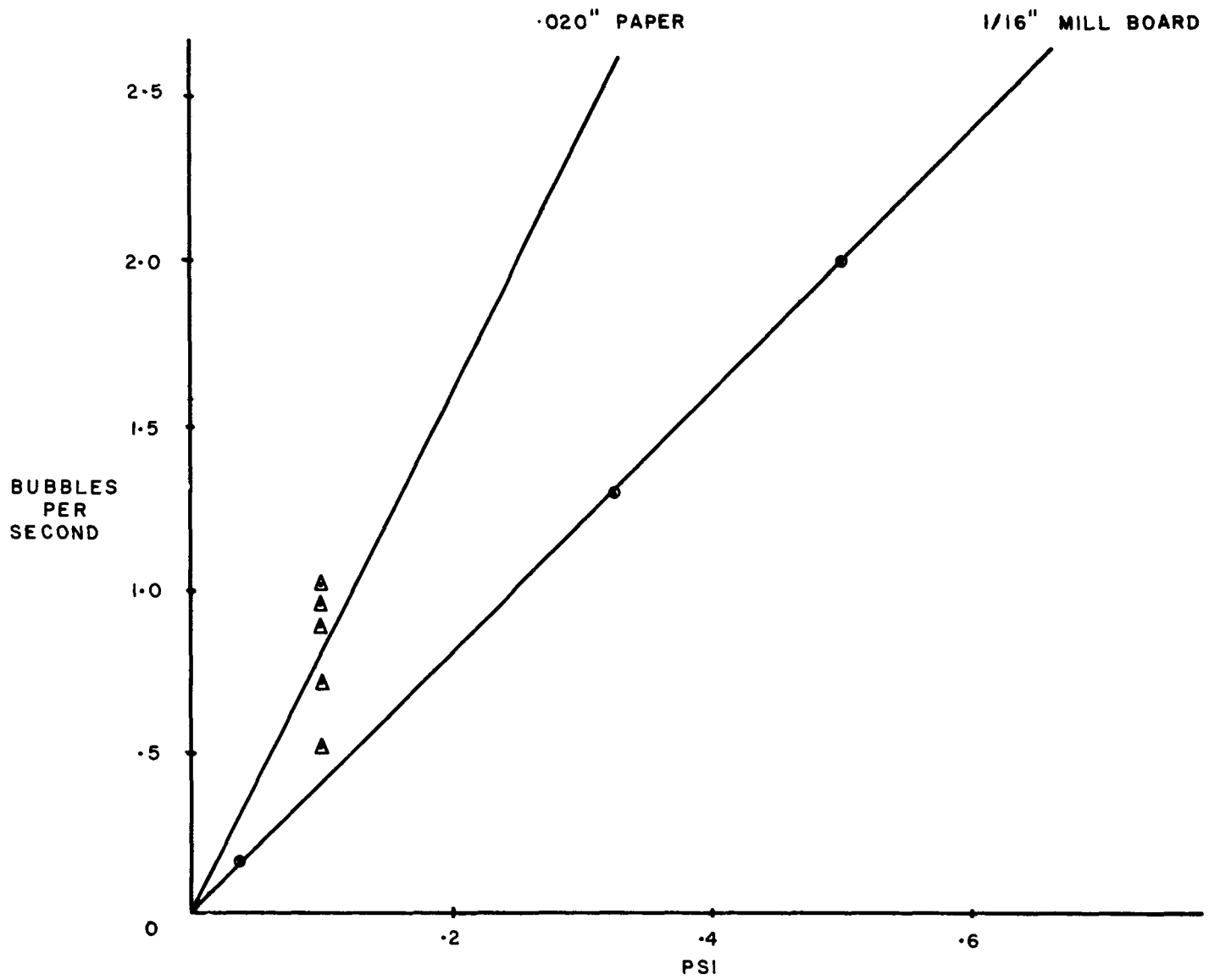
Figure 10. The relationship of air permeation rate and pressure differential across 20-mil and 60-mil thick dry asbestos mats.

Table 2 - Gas Permeability of Dry Asbestos

Specimen No.	Net Pressure (psi)	Flow Rate* (Bubbles/Second)	Ratio Flow Rate psi
1200a	.040	.053	1.32
1200b	.140	.333	2.36
1300	.068	.100	1.47
1400	.061	.043	.71
1500	3.577	.714	.20
2100a	.036	.167	4.64
↓	.324	1.250	3.86
	.504	2.000	3.97
2100b	3.528	1.111	.31
2500	.032	.040	1.25
	.140	.625	4.46
	.324	1.250	3.86
↓	.504	2.000	3.97
3400	.047	.500	10.63
4200a	.036	.167	4.64
4200b	.036	.200	5.56
↓	.144	2.000	13.90
4300	.032	.909	28.41
	.036	1.428	39.65
↓	.054	3.333	61172
4400a	.050	.312	6.24
↓	.144	1.667	11.58
4400b	.032	.007	.22
↓	.144	2.000	13.90
4500	.032	.167	5.22

* This is an arbitrary relative flow rate through a 1-1/4 inch diameter circular area of the mat.
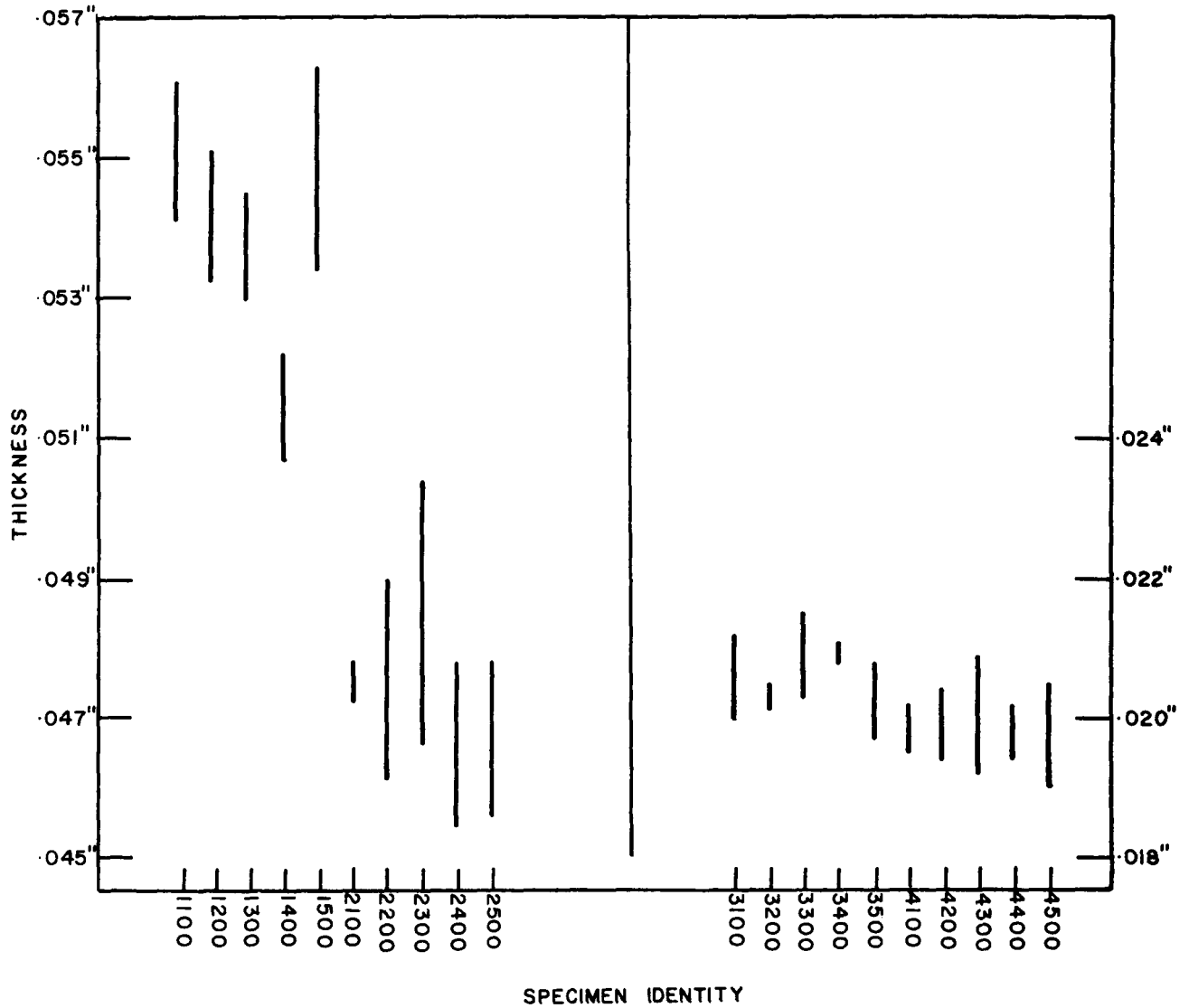
Figure 11. Range of thicknesses measured in 8-1/2 x 11-inch sheets
of 60-mil asbestos board (1000 and 2000 series) and 20-
mil asbestos paper (3000 and 4000 series).

4309A

C. Mat Properties - Wet with KOH

Electrolytic absorption and retention. – This test calls for a measurement of the ratio by weight of 40% KOH solution required to saturate the chrysotile specimen. The saturated specimen is then subjected to an acceleration of 25G for 2 minutes, and the loss of KOH solution is determined. We learned immediately that the saturated chrysotile paper or millboard is much too fragile to survive the manipulations specified by Cooper and Fleischer*. They recommend that the over-saturated specimen be carefully drawn across the clean surface of a glass plate until it ceases leaving a trail of droplets of solution. However, the saturated chrysotile has not sufficient coherence and too much adherence to the plate, and it invariably tears.

In the procedure we adopted, the dry specimen is placed on a rectangle of nichrome screen slightly longer and wider than the specimen. Both are then weighed in a previously weighed plastic cup, to the cover of which is fastened a folded disk of filter paper. The specimen, on the screen, is then placed in a shallow puddle of KOH solution and permitted to become saturated by upward capillarity. We hope, by this procedure, to prevent entrapment of air pockets within the specimen. When the upper surface appears saturated, several drops of additional KOH solution are placed on the specimen, and after the surface excess is absorbed, the specimen (still on the wire screen) is placed on a sheet of dry filter paper and moved repeatedly to a new dry location until the free excess electrolyte has been transferred. With careful handling, the filter paper touches only the lower surface of the supporting screen, and therefore presumably absorbs only the free liquid.

The saturated specimen, with its support screen, is weighed again inside the covered plastic cup (Figure 12). It is then subjected to acceleration of 25G for two minutes and returned to the weighing cup. A piece of the weighed filter paper is used to swab out the specimen holder and recover any KOH solution adhering to the specimen chamber walls; this piece of filter paper is placed in the cup and weighed with the specimen. From the several weighings, we derive the weight of the dry specimen, the saturated specimen, and the liquid retained during the centrifuge treatment.

A low speed centrifuge was built from a motor, speed reducer, and standard Unistrut channel and brackets. Based on the nominal speed of the motor reducer unit, the beam, specimen support bracket, and counter weights were mounted. Then the rotary speed was measured at 358 rpm. The specimen bracket was then adjusted to place the specimen at the proper distance (17. 42 cm) from center. The centrifuge, without its protective shield, is shown in Figure 13.

---

*J. E. Cooper and A. Fleischer, editors, Characteristics of Separators for Alkaline Silver Oxide Zinc Secondary Batteries, Air Force Aero Propulsion Laboratory, 1964, ASTA N64-30013.
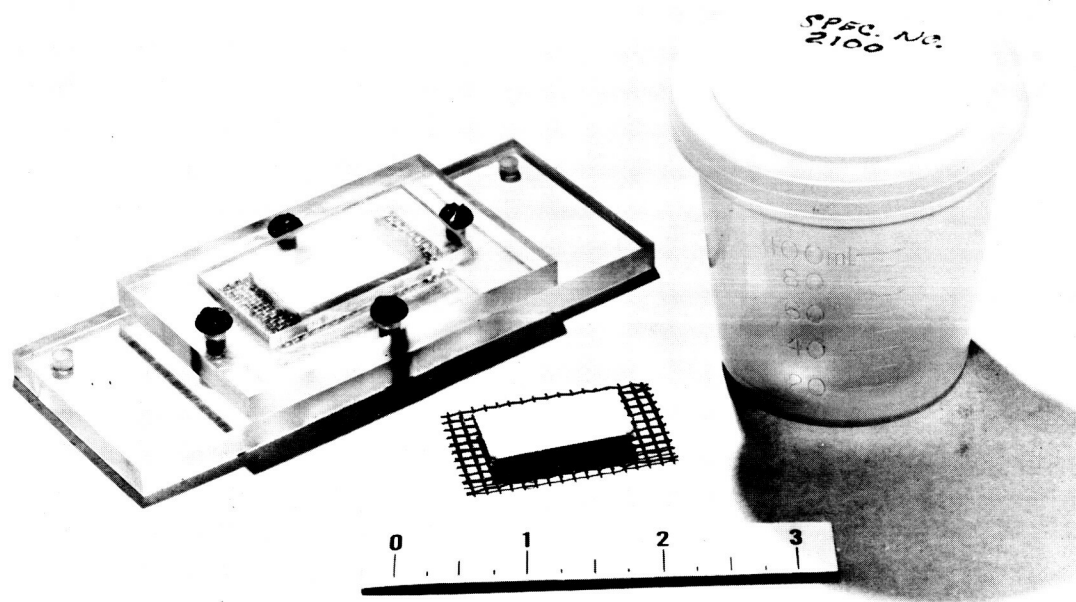
Figure 12.   Specimen and holder for electrolyte absorption and
retention tests.

4307A

Figure 13.   Centrifuge for electrolyte retention tests.

4306A

The data from these tests is summarized in Table 3. Despite the fact that specimens from each series were picked at random, the data are reasonably coherent. The ratio of electrolyte required to saturate the 60-mil millboard is significantly greater than that required for the 20-mil paper. However, the saturated millboard consistently loses a small amount of the electrolyte under 25G acceleration, where the loss by the paper is practically zero.

Perhaps the most interesting aspect of these results is that the millboard absorbs about 5.7 times its weight; the paper, only 3.8 times its weight. This difference is probably attributable to the fact that the paper is compressed by rolling whereas the millboard is not. The millboard swells freely upon absorption of the KOH solution whereas the paper is apparently restrained by the closer interlocking of fibers induced by pressure rolling.

Liquid permeability. – This test procedure was based on the description by Cooper and Fleischer with several modifications. The test consists in measuring the rate of water flow through a known face area of the specimen under a known pressure differential. The specimen is mounted against a supporting screen, and a circular area (1/2 inch diameter) is exposed to the water. From the chamber behind the specimen, a glass tube extends vertically about 4 feet. Near its top are two reference marks 10 cm apart and containing 1.120 ml of water between them. These features are presented schematically in Figure 14.

The specimen of sheet or millboard is cut about 1 inch in diameter to provide a rim area for mounting. This rim was saturated with melted paraffin wax to effect a positive seal to prevent liquid leakage through the edges. The specimen was mounted loosely in the holder and then saturated with water, after which the clamping ring was secured tightly. The holder was then filled with water, coupled to the vertical glass water column, and immersed to a pre-determined depth in a beaker filled to overflowing with water. The two reference marks on the column were thus 114.4 cm and 124.4 cm (average = 119.4 cm) above the level of water in the filled beaker.

The vertical column was then filled with water, and the time required for the surface level to fall between the reference marks was measured. All the dimensions in the test are arbitrary, therefore, the method can serve only as a means of comparing specimens.

Table 3 – Electrolyte Absorption and Retention Under 25 G Acceleration

Spec. No.	Wt. of Spec. gm	Wt. of Absorbed Soln., gm	Wt. Ratio Absorbed	Wt. of Retained Soln., gm	Wt. Ratio Retained
1100	0.5674	3.3970	5.98	2.9034	5.12
1200	0.5250	3.1424	5.99	2.7855	5.31
1300	0.5491	3.0519	5.56	2.6844	4.89
1400	0.5371	2.7296	5.09	2.5925	4.83
1500	0.5470	3.0531	5.57	2.5955	4.74
		Average	5.64		4.98
2100	0.4611	2.5515	5.53	2.2699	4.93
2200	0.4411	2.4119	5.46	2.2976	5.22
2300	0.4499	2.6325	5.84	2.3367	5.20
2400	0.4535	2.6473	5.84	2.3108	5.09
2500	0.4148	2.3924	5.76	2.1640	5.22
		Average	5.69		5.13
3100	0.2245	0.8534	3.80	0.8534	3.80
3200	0.2280	0.8980	3.94	0.8633	3.79
3300	0.2207	0.7999	3.63	0.7852	3.56
3400	0.2186	0.8520	3.90	0.8512	3.89
3500	0.2301	0.8978	3.90	0.8978	3.90
		Average	3.83		3.79
4100	0.2187	0.8425	3.86	0.8443	3.86
4200	0.2153	0.8013	3.73	0.8015	3.73
4300	0.2229	0.8526	3.82	0.8327	3.74
4400	0.2163	0.8035	3.71	0.7957	3.68
4500	0.2138	0.8452	3.95	0.8076	3.77
		Average	3.81		3.76
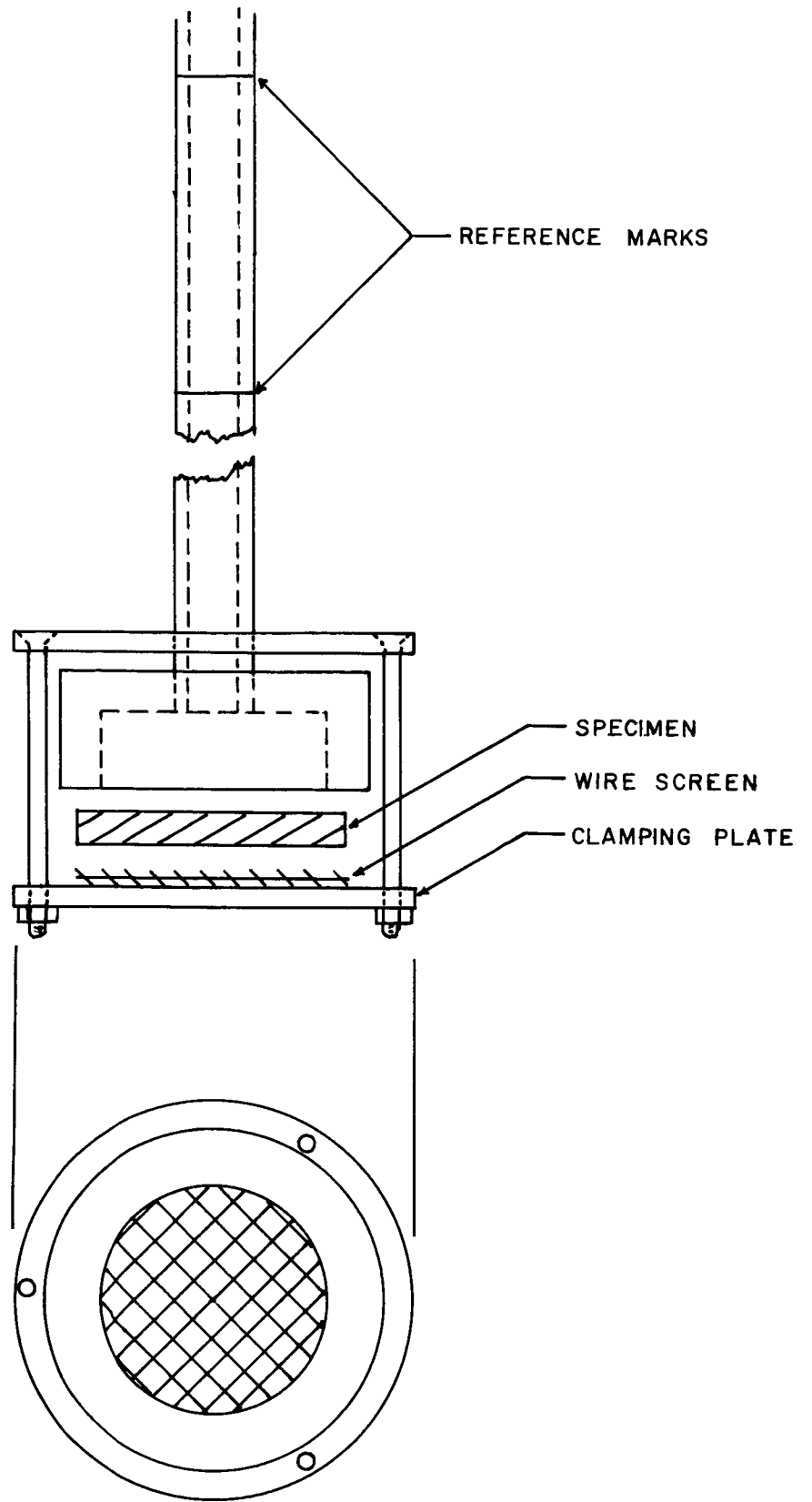
Figure 14. Schematic of specimen holder used for liquid permeability tests.

As described by Cooper and Fleischer, if one assumes that the asbestos mat is essentially a packing of cylindrical tubes with the axes all transverse to the plane of the mat, then, with incorporation of additional data, one may compute a numerical value of porosity of the specimen. However, this computation involves several idealizing assumptions that are not even remotely realized in asbestos mat, and consequently the porosity value so derived is fictitious. Since the liquid permeability test is being surveyed in this program merely as a convenient means of comparing specimens of asbestos for service as a matrix, we believe that the computation of porosity values is an unwarranted elaboration, and we report only the raw data.

The first tests with asbestos specimens yielded grossly erratic results, evidently because of entrapment of air pockets. When the specimens were permitted to saturate by capillary absorption upward from the lower surface, the data became much more coherent.

The data (Table 4) reveal that the specimens of the 1000 series (production start) are much less permeable and much more variable than the specimens of the 2000 series (production end). Roughly, the measured times of permeation correlate with the measured thickness of the dry specimens, although in the case of the 1000-series specimens, the permeability variations seem disproportionately great. Moreover, the slight difference in general thickness of the 2000 and 1000-series specimens cannot account for the notable difference between the permeabilities of the two groups.

For comparison, three sheets (8.5 x 11 inches) each of the 1000-series and the 2000-series material were weighed, and the following results were obtained:

1000 series	214. 0g
2000 series	181. 3g
Difference	32. 7g (or about 15%)

Thus, the weight difference corresponds roughly with the difference in thickness between the two lots of millboard. However, the variation in water permeation rates is greater than that predicted from an exponential dependence on mat thickness. Evidently, the water permeation rate does reveal mat differences more significant than simple thickness or geometric density differences.

Table 4 - Liquid Permeability Tests

Specimen	Specimen Thkns. (inch)	Flow Time (sec.)*
1100	0.0565	978
1200	0.0538	719
1300	0.0537	586
1400	0.0532	732
1500	0.0550	795
2100	0.0494	362
2200	0.0470	317
2300	0.0506	352
2400	0.0478	365
2500	0.0483	323
3100	0.0208	42.5
3200	0.0208	39.7
3300	0.0201	39.4
3400	0.0206	40.7
3500	0.0203	41.3
4100	0.0198	43.8
4200	0.0194	41.0
4300	0.0195	38.8
4400	0.0205	39.1
4500	0.0192	39.2

* Time required to flow 1.12 ml. of water through a 1/2 inch diameter circular area of asbestos mat under an average head of 119.4 cm. of water.

<u>Conductivity of the saturated mat.</u> – Electrolytic conductivity of the saturated mat was measured with a cell similar to that described by Cooper and Fleischer. The cell (diagrammed in Figure 15) splits into two identical halves. Each of these pieces was machined from a Teflon block. When the specimen, with edges sealed by melted paraffin, is clamped between the halves, it presents a circular area of 1/2 inch diameter to the electrolyte.

The reference electrodes in these tests were hydrogen-generating electrodes operating in the same electrolyte that filled the working cell. A Sorensen potentiostat furnished current controlled at 141 ma (which is equivalent to 100 amp./sq. ft. at the specimen surface.)

The test procedure follows: with zero current between the working electrodes, the rheostats in the reference electrode supply circuits were adjusted for gentle production of hydrogen and for zero potential difference between the two reference electrodes. Then, with 141 ma passing through the specimen, the potential difference between the reference electrodes was measured.

Finally, the electrolyte was removed, the specimen was flushed out of the cell by a stream of water, the electrolyte was replaced, and the resistance of the electrolyte alone was measured. The latter constitutes a blank measurement, but its relationship to the specimen measurement is very dubious. The distance of separation between the two Luggin capillary orifices is determined by the thickness of the compressed rim of the specimen, whereas the rest of the specimen mat expands freely to several times its dry thickness. Therefore, the mat resistance measured in this apparatus pertains strictly only to this particular condition of the mat and may not be applied unchanged to different situations. For that reason, the "blank" values are reported in Table 5, but are not incorporated in the measured values for the specimens. Since the current density is regulated at 100 ASF, the potential across the specimen is converted to ohms per square foot by applying the factor 10^{-2}.

The difference in resistance of the 1000 and 2000-series correlates qualitatively with the measured thicknesses of the dry mat, and also with the measured weights of the dry mats (cf. thickness measurement and liquid permeability tests).
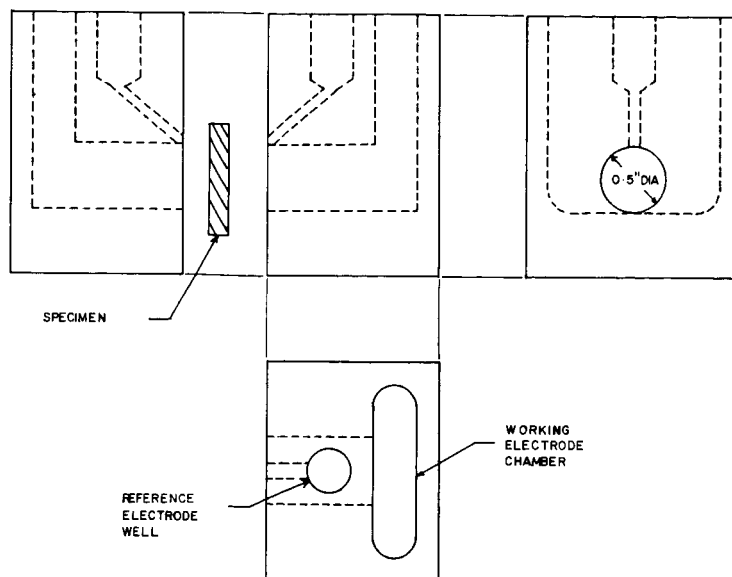
(a)
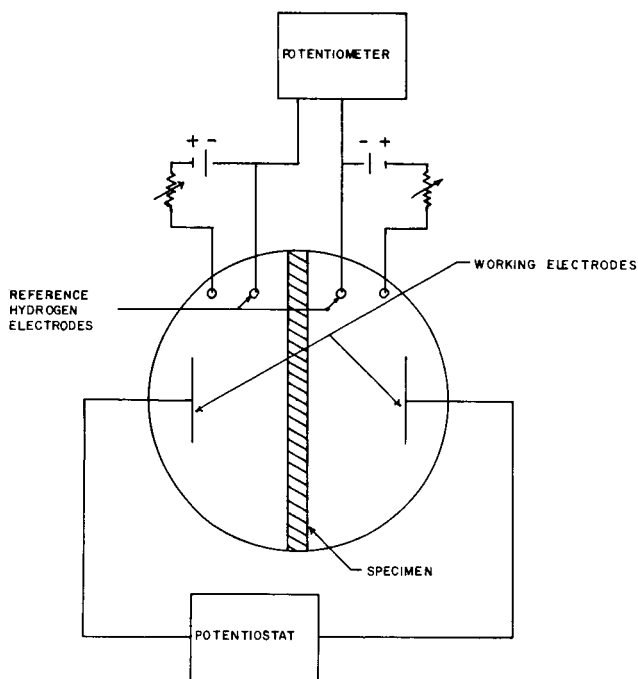
(b)

Figure 15. (a) Diagram of cell used for electrolytic conductivity
            measurements.
            (b) Electrical schematic of conductivity apparatus.

Table 5 – Electrolytic Resistance

Specimen	Δ E, Volts	R, ohm/ft^2
1103	0.1081	10.81×10^{-4}
1203	0.1083	10.83
1303	0.1081	10.81
1403	0.0835	8.35
1503	0.1088	10.88
2103	0.0891	8.91
2203	0.0843	8.43
2303	0.0905	9.05
2403	0.0917	9.17
2503	0.0874	8.74
3103	0.0466	4.66
3203	0.0695	6.95
3303	0.0541	5.41
3403	0.0667	6.67
3503	0.0508	5.08
4103	0.0400	4.00
4203	0.0574	5.74
4303	0.0445	4.45
4403	0.0659	6.59
4503	0.0561	5.61
Blank	0.0355	
Blank	0.0350	
Blank	0.0373	

Gas permeability of wet mat. – The air permeability was measured for specimens of the asbestos mats containing absorbed 40% KOH solution in the weight ratio 1 : 1 and increasing to saturation. For this purpose, the apparatus at hand was modified to improve its sensitivity. The specimen, with edges sealed by melted paraffin, was mounted in a holder which supplied air under measured pressure to the lower surface of the specimen. A 1-1/4 inch diameter circular area of the specimen was exposed to the test gas. The gas permeating the specimen was contained by an upper chamber of the holder and conducted to a water bubbler, which served to indicate and measure the gas flow. In the holder, the specimen was restrained against the pressure differential by a metal screen directly above it.

Preliminary experiments with bubbler design to achieve maximum sensitivity as a gas flow meter revealed several interesting considerations. With decreasing orifice size, the bubble becomes smaller, but the capillary forces within the bubbler tube make necessary greater gas pressures to expel a bubble of gas. In fact, with a very small diameter tube, the gas is released as a burst of bubbles. The optimum condition was attained by using a tapered polypropylene tube to minimize capillary effects and trimming off the tapered end to obtain the optimum orifice diameter.

Pressure of the air supplied to the specimen was measured by either a water manometer, a mercury manometer, or a Bourdon gage, depending on the pressure. This provided accurate pressure measurements ranging from a fraction of an inch of water to 30 psig. Very low pressures were corrected for the depth of immersion of the bubbler tip (about 1 inch).

The data are recorded in Table 6. Probably the most significant yield from these tests is the gross difference between the paper and millboard. The 20-mil paper specimens consistently leaked gas at low pressure differentials (about 10 inches of mercury) even when saturated with KOH solution. On the other hand, the 60-mil millboard usually was impermeable at 30 psi even at the minimum (1 : 1 weight ratio) content of KOH solution.

We observed that in all cases the gas pressure forced KOH solution out onto the top surface of the specimen. When the pressure differential was relaxed, the free solution was quickly reabsorbed into the specimen.

Table 6 – Gas Permeability of Wet Asbestos

Specimen Identity and Electrolyte Ratio		Net Pressure (psi)	Flow Rate* (Bubbles/Sec)	Specimen Identification		Net Pressure (psi)	Flow Rate * (Bubbles/Sec)
1201	1:1	6.958	.023	1501	2:1	25.0	.143
		8.526	.025			25.0	.125
		9.065	.028			25.0	.111
		9.408	.045	2101	1:1	3.283	.059
	2:1	11.270	.019			4.949	.083
		14.308	.014			7.448	.125
		15.500	.018			12.005	.250
		16.000	.014		2:1	10.241	.050
	3:1	25.000	.032			12.225	.071
		30.000	.008			14.700	.091
1202	1:1	1.421	.071			17.500	.143
		1.667	.100			20.000	.167
		1.764	.100		3:1	17.500	.033
	2:1	7.105	.038			20.000	.040
		9.898	.043			25.000	.071
		14.700	.067		4:1	17.500	.016
		15.000	.062			20.000	.023
		17.500	.067			25.000	.045
		20.000	.071	2102	1:1	21.500	.167
		22.500	.083			18.000	.333
		25.000	.091		2:1	19.000	.077
		27.500	.100		3:1	30.000	0.000
		30.000	.111	2501	1:1	3.283	.100
1301	1:1	1.862	.020			2.009	.250
		2.891	.028			1.911	.250
		3.675	.037		2:1	5.047	.050
		4.116	.037			25.500	.023
		4.214	.040	3401	1:1	.418	.036
		4.214	.042			.526	.034
	2:1	30.000	0.000			.814	.050
1401	1:1	30.000	0.000			.900	.040
1501	1:1	3.773	.048		2:1	1.176	.048
		2.646	.333			1.372	.056
		3.773	.500			1.372	.050
		3.822	.083		3:1	1.519	.050
	2:1	6.223	.143			1.813	.053
		10.535	.125			2.107	.059
		18.500	.143		4:1	2.597	.059
		21.000	.143			2.989	.062
3401	4:1	3.381	.067	4402	2:1	12.250	.143
	5:1	3.185	.056		3:1	7.840	.071
		3.675	.056			12.250	.143
		4.018	.056		4:1	12.000	.100
4201	1:1	.378	.067			12.000	.100
		.400	.067			20.000	.333
		.428	.071	4403	1:1	.407	.024
	2:1	.875	.031			.684	.037
		1.001	.029			.864	.043

Table 6 (Cont'd)

Specimen Identity and Electrolyte Ratio		Net Pressure (psi)	Flow Rate* (Bubbles/Sec)
4201	2:1	1.372	.031
	3:1	1.667	.033
		2.156	.034
		2.500	.034
	4:1	3.234	.032
		3.578	.028
		4.655	.031
4301	1:1	.119	.031
		.328	.042
		.911	.043
		5.635	.200
		9.800	.500
	2:1	.846	.013
		3.773	.040
		7.350	.125
		12.495	.200
4401	1:1	2.009	.011
		4.900	.021
		7.350	.033
		9.800	.050
		12.250	.071
	2:1	30.000	0.000
	3:1	18.000	.143
		18.000	.125

Specimen Identification		Net Pressure (psi)	Flow Rate* (Bubbles/Sec)
4403	1:1	2.450	.143
		7.350	.454
		12.250	.833
	2:1	2.646	.100
		7.399	.333
		12.225	.556
	3:1	4.753	.043
		7.350	.077
		12.225	.167
	4:1	5.978	.053
		7.350	.071
		12.225	.200
4501	1:1	.040	.167
		.043	.333
	2:1	.302	.091
		.367	.100
		.608	.143
	3:1	.504	1.667
4402	1:1	.972	.016
		2.450	.040
		4.900	.083
		10.045	.250
	2:1	2.205	.020
		4.900	.043

* This is an arbitrary relative flow rate through a 1-1/4 inch diameter circular area of the mat.

We suggest the following very tentative interpretation. At the 1:1 weight ratio of asbestos to KOH solution, the paper contains only one-fourth the saturating quantity of solution, the millboard contains only one-sixth. Evidently, the millboard structure is such that the pressure-induced migration of some liquid produces a saturated and sealed zone near the low pressure side. For some reason, the structure of the 20-mil paper or its lack of sufficient thickness does not permit a sealed zone to develop.

D.   Chemical Degradation

These degradation tests consist in maintaining specimens in KOH solution of 30, 40, 50, and 60 weight percent concentration for 100 and 1000-hour periods at temperatures of 50, 100, 150, and 200°C. Tests at 50°C in 50 and 60% KOH and at 200°C in 30 and 40% KOH are not required because these represent nonequilibrium concentration-temperature combinations for the KOH.

The tests were performed in ordinary laboratory ovens which incorporate thermostat controls. As containers, we used 4 ounce Teflon FEP bottles with screw caps. These were satisfactory at the two lower temperatures, but would not retain the water at 150 and 200°C. We then sealed each bottle individually in a capsule made from standard 2 inch threaded pipe nipples, closed with the threaded caps. We used Teflon pipe tape for a thread sealant, and learned that only certain premium brands of Teflon tape are effective, and only when seven or eight laps of the tape are applied to the thread. The caps were then tightened with a large pipe wrench, the handle of which was lengthened with a four-foot pipe.

The Teflon bottles were weighed empty and with the specimens of asbestos. A polonium-activated dust brush was placed in the balance case to speed the equalization of static charges which are specially troublesome with this plastic. A volume of 50 ml of the KOH solution was placed in the bottle. Where 60% KOH was to be used, the appropriately weighed quantity of dry KOH pellets and volume of water were placed in the bottle. At the end of the test, the contents of the bottle were transferred quantitatively to a 600 ml beaker, diluted with much water and permitted to settle. The supernatant liquid was decanted through a sintered glass filter, and the washing was repeated. The final wash was very slightly acidified with HCl to facilitate complete removal of KOH, and the solid was transferred to the filter, dried, and weighed.

For the lower temperature tests, the bottles were capped tightly and placed in the oven. For the higher temperature tests, the bottles were capped lightly and placed in the pipe capsule, 1 ml of water was introduced to provide balancing vapor pressure, and the top cap was installed. Each capsule was then weighed to the nearest 0.1g and placed in the oven. After several days, the capsules were removed, allowed to cool, and weighed again. If there was any significant loss, the capsule was opened, a new sample was prepared and resealed in the capsule. Only those specimens that showed negligible weight loss were accepted as valid tests.

As a result of the difficulty encountered in achieving a positive vapor seal, the tests at higher temperatures were delayed several weeks. At the time of this reporting, the 1000 hour tests at 150°C are incomplete. However, the 100 hour tests are complete, and they probably reveal that the chrysotile cannot survive even the shorter test period at high temperatures. The quantitative results are recorded in Table 7.

As expected, the dissolution of specimens is greater and faster with increasing time, temperature, and concentration of the KOH. However, with the exception of two tests and the results for the 1000 hour, 200°C tests, the weight losses attain a limit of about 40%. This value corresponds quite well with the value predicted (44%) on the assumption that the chrysotile is converted completely to insoluble $Mg(OH)_2$ and soluble silicate. If this assumption is valid, the data indicate that the conversion of chrysotile to $Mg(OH)_2$ or hydrated MgO is virtually completed in 1000 hours at 100°C and in 100 hours at 150°C.

The data reveal that natural chrysotile is probably not a satisfactory matrix for long service at temperatures as high as 100°C. The tests suggest, however, that the insoluble residue, if it retains a satisfactory fibrous structure, may be superior to chrysotile. We shall test this hypothesis during the second phase of the program.

E. Electrochemical Degradation

This test consists essentially in subjecting the specimen to a current density of 40 ASF in 40% KOH electrolyte at 100°C for 72 hours. At 24 hour intervals, 1 ml samples were drawn of the anolyte and catholyte, and the electrodes were washed with nitric acid to remove any deposits. The electrolyte specimens and electrode washings were then analyzed spectrographically for identity and quantity of constituents of the asbestos mat.

Table 7 – Chemical Degradation Test at 50°C

Test Hrs.	% KOH	Spec. Ident.	Wgt. of Spec., gm	Wgt. of Recovered Residue, gm	Wgt. Loss, gm	% Wgt. Loss
100	30	1600	1.9337	1.8785	0.0552	2.85
100	30	2600	1.5821	1.5640	0.0181	1.14
100	30	4600	1.7163	1.6110	0.1053	6.14
100	40	3600	1.7833	1.6996	0.0837	4.70
100	40	3600	1.8672	1.7740	0.0932	5.00
100	40	3600	1.7350	1.6425	0.0925	5.33
1000	30	2600	1.6733	1.6226	0.0507	3.00
1000	30	2600	1.8615	1.8240	0.0375	2.00
1000	30	4600	1.9140	1.8123	0.1017	5.31
1000	40	1600	1.6739	1.6150	0.0589	3.52
1000	40	1600	1.6958	1.6016	0.0942	5.56
1000	40	4600	1.8163	1.7144	0.1019	5.61

Chemical Degradation Tests at 100°C

Test Hrs.	% KOH	Spec. Ident.	Wgt. of Spec., gm	Wgt. of Recovered Residue, gm	Wgt. Loss, gm	% Wgt. Loss
100	30	1600	1.0323	0.9556	0.0767	7.50
100	30	2600	1.0000	0.9233	0.0767	7.67
100	30	3600	1.1234	1.0634	0.0600	5.30
100	40	1600	1.0670	0.9533	0.1137	10.70
100	40	3600	1.3561	1.2240	0.1321	9.75
100	40	4600	1.2826	1.1524	0.1302	10.14
100	50	1600	1.1248	0.9386	0.1862	16.55
100	50	2600	1.0361	0.8830	0.1531	14.75
100	50	4600	1.2951	1.0834	0.2117	16.35
100	60	2600	1.2345	1.0381	0.1964	15.90
100	60	3600	1.0240	0.6879	0.3361	32.85
100	60	4600	1.3108	1.0752	0.2356	17.97
1000	30	1600	2.0227	1.7721	0.2506	12.30
1000	30	1600	1.9937	1.5516	0.4421	22.20
1000	30	4600	1.1727	0.7428	0.4299	36.6
1000	40	2600	2.2666	1.5260	0.7406	32.80
1000	40	3600	1.3996	0.8202	0.5794	41.40
1000	40	3600	1.3334	0.9307	0.4027	30.2
1000	50	2600	2.2110	1.3054	0.9056	41.00
1000	50	3600	1.3133	0.9247	0.3386	29.6
1000	50	4600	1.2155	0.7722	0.4433	36.5
1000	60	1600	2.0651	1.2472	0.8179	42.00
1000	60	2600	2.0825	0.7973	1.2852	62.75
1000	60	4600	1.2282	0.7553	0.4729	36.9

Chemical Degradation Tests at 150°C

Test Hrs.	% KOH	Spec. Ident.	Wgt. of Spec.,gm	Wgt. of Recovered Residue,gm	Wgt.Loss,gm	% Wgt. Loss
100	30	1600	1.6288	1.5707	0.0581	3.6
100	30	3600	1.0801	0.8972	0.1829	16.9
100	30	4600	1.0879	0.9204	0.1675	15.4
100	40	1600	1.4339	1.4046	0.0293	2.0
100	40	2600	1.2313	1.0146	0.2168	17.6
100	40	4600	1.0652	0.8265	0.2387	22.4
100	50	1600	1.2260	0.8495	0.3765	30.7
100	50	2600	1.2984	0.8898	0.4086	31.5
100	50	3600	1.1061	0.6652	0.4409	39.9
100	60	2600	1.3376	0.9040	0.4336	32.4
100	60	3600	1.3302	0.8137	0.5165	38.8
100	60	4600	1.2238	0.5945	0.6293	51.4

Chemical Degradation Tests at 200°C

Test Hrs.	% KOH	Spec. Ident.	Wgt. of Spec.,gm	Wgt. of Recovered Residue,gm	Wgt.Loss,gm	% Wgt. Loss
100	50	1600	1.2442	0.7935	0.4507	36.2
100	50	2600	1.1693	0.7425	0.4268	36.5
100	50	4600	1.0168	0.6443	0.3725	36.6
100	60	2600	1.1065	0.6902	0.4163	37.6
100	60	3600	1.1940	0.7335	0.4605	38.6
100	60	4600	1.0891	0.6580	0.4311	39.6

These tests were performed in a V-shaped cell machined from a Teflon block (Figure 16). In one leg of the cell was a shoulder to support a platinum wire screen, on which the specimen rested. Since the specimen was located below the electrode level, the electrolytic gases escaped without entering the specimen.

The cell was placed in a laboratory drying oven at 100°C. Electrolytic hydrogen was vented through a tube to the exterior of the oven, and oxygen was vented into the oven. The requisite current (0.27 amp) was provided by a Sorensen potentiostat.

At this time, the spectrographic analysis of all the specimens is not complete, but some qualitative information has been obtained. The 40% KOH solution purified electrolytically for these tests contained, as revealed by spectrography, very small concentrations of magnesium, calcium, and aluminum ions. These, of course, will not be removed by electrolysis. The several samples of used electrolyte analyzed were those taken at the ends of the 72 hour tests, when the soluble impurity concentrations were greatest. The concentrations of Mg, Ca, and Al ions were no greater than in the original electrolyte. Silicon was only barely detectable.

In the first test, the specimen was the 20-mil paper. At the end of the first 24 hours, there was a visible mottled grey deposit on the anode surface. The deposit did not dissolve in nitric acid. At the end of test (72 hours) the deposit was apparently unchanged and still insoluble in nitric acid. After standing overnight in the KOH electrolyte, the grey material changed to a golden brown color which dissolved in nitric acid. Upon evaporation to dryness a very small quantity of brown residue appeared. It dissolved readily in a drop of hydrochloric acid, which was then analyzed and proved to contain iron.

Three subsequent tests were performed with 60-mil millboard specimens. During the first two of these tests, the electrodes remained bright and clean, and the electrolyte specimens revealed no significant concentrations of constituent elements of the asbestos. During the last test (specimen 2600), very small amounts of brown deposit were formed on the anode. This material was readily soluble in nitric acid. Analysis of this also showed the presence of iron.

These data seem to indicate the deposition on the anode of the black Fe_3O_4 which, upon standing at room temperature for several hours, converts to the red Fe_2O_3. The appearance of iron at the anode is remarkable in view of our observation that iron is not present in the anolyte in spectrographically significant concentration.
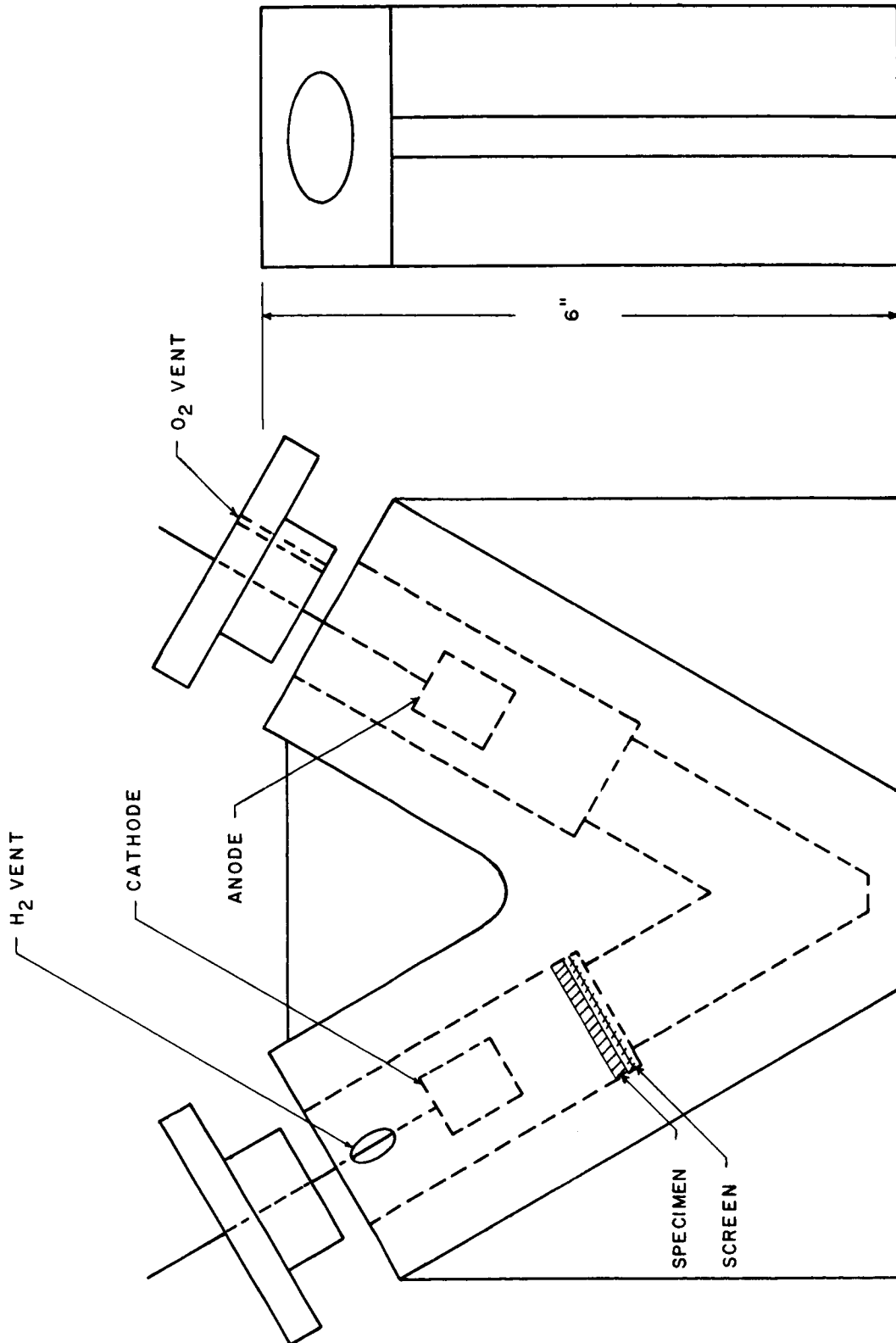
Figure 16. Schematic diagram of V-cell used for electrochemical degradation tests.

4305A

DISCUSSION AND CONCLUSIONS

Some summary comments are in order here with regard to an overall view of the test results reported above and how they relate to the function of a fuel cell matrix. Of particular interest will be how these results can serve as a baseline against which to measure alternate materials to be tested in the next phase of the program.

Asbestos Properties

The first set of tests on the asbestos were those which described the basic material properties - specifically the composition, fiber structure, and surface area of the asbestos. The most significant factor in the composition of asbestos is the iron impurity (about 0.85% Fe_2O_3 by weight). During the electrochemical tests, iron was the only material detected in the residue formed on the electrodes of the electrolysis cell. It is evident, therefore, that iron can be preferentially leached from the asbestos and transported to the electrodes (primarily to the anode) during cell operation. This can be a possible source of catalyst poisoning in cells containing an asbestos separator. It is concluded that prospective separator materials should not contain iron. If raw materials do contain iron compounds, the iron should be removed before the material is used as a cell separator.

The detailed fiber morphology and surface area characteristics of asbestos serve to describe some details of the asbestos structure, but there is no apparent reason that these characteristics of asbestos can serve as a standard against which to measure the desirability of alternate materials. It is most likely that the extremely small fiber diameter of the asbestos is not required for the attainment of satisfactory properties in a cell separator. This seems particularly true when it is noted that most of the asbestos fibers appear to be present in the mat as fiber bundles rather than as separate fibers.

Dry Mat Properties

Many of the properties of the dry asbestos mat also fall into the category of primarily describing asbestos rather than serving as a criterion for alternate materials. The tensile strength of asbestos mats is one of these properties. The tests performed illustrated the effect of fiber orientation and gave some idea of sheet-to-sheet reproducibility. However, these tests appear to be nondiscriminating in determining if a given sheet of asbestos would serve as a satisfactory separator. In the dry state, the asbestos mat is fragile but is strong enough to be handled so that it can be assembled into a cell. In the wet state, it loses most of even this strength. It still, however, can apparently be accommodated in present cell designs. In searching for improved materials, it would be hoped that any new material would have at least the strength of the present asbestos mats (both wet and dry), and any improvement in strength would certainly be an advantage.

The porosity of the dry asbestos mats were measured as approximately 70 percent. However, when the mat is wet with electrolyte, it swells several-fold so that the effective porosity in the operating mat probably exceeds 90 percent. This high porosity does represent one of the chief advantages of asbestos, and it may be difficult to find another material that can be fabricated into a coherent structure with this high a porosity.

Wet Mat Properties

The properties of the asbestos mat when wet with the KOH electrolyte were the most significant tests conducted in this program. The ionic conduction, electrolyte absorption-retention, gas permeability, and the chemical and electrochemical degradation tests all revealed information which will be of great interest in comparing alternate materials to these chrysotile asbestos mats.

The resistance to ionic conduction of the asbestos mats ranged from about 2 to 3 times that of the free electrolyte. Since this internal IR drop represents an efficiency loss in an electrochemical cell, this property is an important one in determining the desirability of a matrix material. This property is determined by the porosity and pore size of the separator material. Since it may be difficult to obtain materials with porosity as high as asbestos, the attainment of a desirable value of ionic conductivity can be pursued in other materials by the dual control of porosity and pore size.

The high effective porosity of asbestos was again manifested in the electrolyte absorption and retention tests. The 20-mil asbestos paper absorbed about 3.8 times its weight in electrolyte, and the 60-mil millboard soaked up about 5.7 times its weight. The good wettability (low contact angle) by KOH, and a small pore size in the asbestos was evidenced by the fact that very little of the electrolyte could be removed from the asbestos under a load of 25G's. These properties should be of particular interest in a regenerative cell in which a large electrolyte capacity in the separator material is desired. The excellent retention of the electrolyte under load also indicates that the pore size is sufficiently small so that some increase in pore size could possibly be afforded. The resultant sacrifice of electrolyte retention properties might be more than compensated by a decrease in the resistance to ionic conduction in the mat.

The studies of gas permeation through wetted mats also indicate the pore structure of the asbestos. Of particular interest was the good sealing properties of the 60-mil millboard compared to the 20-mil paper. The 20-mil paper had a very low bubble pressure even when saturated, whereas the 60-mil material was "leak tight" with a liquid content of less than one-fifth of its saturation value. It is possible that the vertical fibers of the wool belt on which the 20-mil paper is processed leave "pin-holes" in the paper which become subsequent leakage paths. The thicker millboard, which is made up of multiple layers of this material transferred from the wool belt, would not have these pin holes extend through the entire laminated sheet. Since the cell separator should not allow passage of gas through it during cell operation, the gas permeation test is a critical one. This property will be an important criterion for suitability of a cell separator material.

The electrolytic degradation tests yielded very little positive information other than the appearance of iron oxide, principally on the anode, as discussed above. The significance of these tests seems to be that the electrolyte after electrolysis contained no measurable amounts of contamination from the asbestos although iron was being transferred to the electrodes. However, we plan to repeat these tests with more critical spectrographic techniques before considering this analysis final.

The limiting feature of asbestos for cell separator use seems to be a straight forward lack of chemical compatability with the electrolyte. The chemical degradation tests show that at 150°C and over, the asbestos appears to lose weight until about 40% of the weight of the starting material is dissolved at which time the remaining material is stable. This observation will

be verified by completion of long-time tests now in progress. However, it seems likely that this weight loss is attributed to the silica being leached out of the asbestos leaving a stable $Mg(OH)_2$ residue. The use of asbestos, therefore, definitely seems limited to temperatures in the 100°C range and lower if long-time usage is required. Tests will be performed on chemically degraded asbestos to determine if, in fact, a stable $Mg(OH)_2$ material is formed. If it is, then the fibrous $Mg(OH)_2$ that will be examined in the next phase of this program may prove to be a very promising material for high-temperature use in KOH electrolytes.

This summary discussion has not meant to be an exhaustive discussion of the test results obtained during this phase of the program. Rather its aim has been to highlight certain properties of the asbestos that will be of most interest in comparison with materials to be studied in Task II of the program in a search for an improved cell separator material. Undoubtedly, as this study proceeds, further significance of these results will become apparent in relationship to data obtained on new materials. The final report can then consider these results once more in the framework of a comparison with these other candidate cell separator materials.

DISTRIBUTION LIST

National Aeronautics & Space Administration
Washington, D. C.   20546
Attention: Ernst M. Cohn, Code R NW
         T. Albert, Code MLT
         A. M. Andrus, Code FC

National Aeronautics & Space Administration
Scientific & Technical Information Facility
Post Office Box 33
College Park, Maryland 20740
Attention: NASA Representative
(2 Copies plus 1 reproducible)

National Aeronautics & Space Administration
Goddard Space Flight Center
Greenbelt, Maryland   20711
Attention: Thomas Hennigan, Code 716. 2

National Aeronautics & Space Administration
Langley Research Center
Langley Station
Hampton, Virginia   23365
Attention: S. T. Peterson

National Aeronautics & Space Administration
Lewis Research Center
21000 Brookpark Road
Cleveland, Ohio   44135
Attn: B. Lubarsky, MS 500-201
      M. J. Saari, MS 500-202
      H. J. Schwartz, MS 500-202
      J. E. Dilley, MS 500-309
      N. D. Sanders, MS 302-1
      Dr. J. S. Fordyce, MS 302-1
      V. Hlavin, MS 3-14 (Final Only)
      Technology Utilization Office, MS 3-19
      D. B. Soltis, MS 500-202
      Library, MS 60-3
      Report Control, MS 5-5

National Aeronautics & Space Administration
Marshall Space Flight Center
Huntsville, Alabama   35812
Attention: Mr. Charles Graff
          R-ASTR-EAP

National Aeronautics & Space Administration
Marshall Space Flight Center
Huntsville, Alabama   35812
Attention: Mr. Richard Boehme
          R-ASTR-E

National Aeronautics & Space Administration
Ames Research Center
Moffett Field, California 94035
   Mountain View
Attention: James R. Swain

National Aeronautics & Space Administration
Ames Research Center
Moffett Field, California   94035
   Mountain View
Attention: Mr. T. Wydeven, Environmental Control Branch

National Aeronautics & Space Administration
Ames Research Center
Moffett Field, California   94035
   Mountain View
Attention: John Rubenzer

National Aeronautics & Space Administration
Manned Spacecraft Center
Houston, Texas 77001
Attention: William R. Dusenbury
          Robert Cohen, Gemini Project Office
          F. E. Eastman (EE-4)
          Hoyt McBryar, EP-5, Bldg. 16

Jet Propulsion Laboratory
4800 Oak Grove Drive
Pasadena, California   91103
Attention: Aiji Uchiyama

Department of the Army

U. S. Army Engineer R&D Labs.
Fort Belvoir, Virginia   22060
Attention: Dr. Galen Frysinger (Code SMOFB-EP)
            Electrical Power Branch

U. S. Army Electronics R&D Labs.
Fort Monmouth, New Jersey 07703
Attention: Code SELRA/SL-PS

Harry Diamond Labs.
Room 300, Building 92
Connecticut Avenue & Van Ness Street, N. W.
Washington, D. C. 20008
Attention: Nathan Kaplan

Army Material Command
Research Division
AMCRD-RSCM T-7
Washington, D. C.   20012
Attention: John W. Crellin
           Marshall Aiken

Natick Labs.
Clothing & Organic Materials Division
Natick, Massachusetts 01760
Attention: Leo A. Spano
            Robert N. Walsh

U. S. Army TRECOM
Physical Sciences Group
Fort Eustis, Virginia 23604
Attention: (SMOFE)

U. S. Army Research Office
Box CM, Duke Station
Durham, North Carolina 27706
Attention: Paul Greer
            Dr. Wilhelm Jorgensen

U. S. Army Mobility Command
Research Division
Center Line, Michigan 48015
Attention: O. Renius (AMSMO-RR)

Department of the Navy

Office of Naval Research
Department of the Navy
Washington, D. C.   20360
Attention: Dr. Ralph Roberts, Code 429

Office of Naval Research
Department of the Navy
Washington, D. C.   20360
Attention: H. W. Fox, Code 425

Bureau of Naval Weapons
Department of the Navy
Washington, D. C.   20360
Attention: Milton Knight, Code RRRE-62

U. S. Naval Research Laboratory
 Washington, D. C.   20390
Attention: Dr. J   C. White, Code 6160

Bureau of Ships
Department of the Navy
Washington, D. C.   20360
Attention: C. F. Viglotti, Code 660

Naval Ordance Laboratory
Department of the Navy
Corona, California 91720
Attention: William C. Spindler (Code 441)

Naval Ordnance Laboratory
Department of the Navy
Silver Springs, Maryland 20910
Attention: Phillip B. Cole (Code WB)

U. S. Navy Marine Engineering Laboratory
Special Projects Division
Annapolis, Maryland 21402
Attention: J. H. Harrison

Department of the Air Force

Flight Vehicle Power Branch
Air Force Aero Propulsion Laboratory
Wright-Patterson Air Force Base, Ohio 45433
Attention: Don R. Warnock (Code APIP-2)

Air Force Cambridge Research Laboratory
Attention: CRZE
L. C. Hanscom Field
Bedford, Massachusetts 01731
Attention: Code CRFE

Rome Air Development Center
Griffiss AFB, New York 13442
Attention: Frank J. Mollura (EMEAM)

Lt. L. S. Harootyan
Energy Conversion Branch
Aero-Propulsion Laboratory
Wright-Patterson Air Force Base, Ohio 45433

Mr. Jesse Crosby, MAMP
Air Force Materials Laboratory
Wright-Patterson Air Force Base, Ohio 45433

Atomic Energy Commission

Army Reactors, DRD
U. S. Atomic Energy Commission
Washington, D. C. 20545
Attention: D. B. Hoatson

Other Government Agencies

Office, DDR&E: USW & BSS
The Pentagon
Washington, D. C. 20301
Attention: G. B. Wareham

Staff Metallurgist
Office, Director of Metallurgy Research
Bureau of Mines
Interior Building
Washington, D. C. 20240
Attention: Kenneth S. Higbie

Mr. D. Bienstock
Bureau of Mines
4800 Forbes Avenue
Pittsburgh, Pennsylvania   15213

Office of Technical Services
Department of Commerce
Washington, D. C.   20009

Clearing House
5285 Park Royal Road
Springfield, Virginia 22151

Private Industry

Aeronutronic Division
Philco Corporation
Ford Road
Newport Beach, California 92663
Attention: Dr. S. W. Weller

Alfred University
Alfred, New York 14802
Attention: Prof. T. J. Gray

Allis-Chalmers Mfg. Company
1100 South 70th Street
Milwaukee, Wisconsin 53201
Attention: Dr. W. Mitchell, Jr.

Allison Division
General Motors Corporation
Indianapolis, Indiana 46206
Attention: Dr. Robert B. Henderson

American Machine & Foundry
689 Hope Street
Springdale, Connecticut 06879
Attention: Dr. L. H. Shaffer
          Research & Development Division

American Cyanamid Company
1937 W. Main Street
Stamford, Connecticut 06901
Attention: Dr. R. G. Haldeman

Aerospace Corporation
P. O. Box 95085
Los Angeles, California 90045
Attention: Tech. Library Document Ctr.

Arthur D. Little, Inc.
Acorn Park
Cambridge, Massachusetts 02140

Atlantic Refining Company
500 South Ridgeway Avenue
Glenolden, Pennsylvania 19036
Attention: Dr. Harold Shalit

Atomics International Division
North American Aviation, Inc.
8900 DeSoto Avenue
Canoga Park, California 91304
Attention: Dr. H. L. Recht

Battelle Memorial Institute
505 King Avenue
Columbus, Ohio 43201
Attention: Dr. C. L. Faust

Bell Telephone Laboratories, Inc.
Murray Hill, New Jersey 07971
Attention: Mr. U. B. Thomas

ChemCell Inc.
3 Central Avenue
East Newark, New Jersey 07029
Attention: Mr. Peter D. Richman

Clevite Corporation
Mechanical Research Division
540 East 105th Street
Cleveland, Ohio 44108

Douglas Aircraft Company, Inc.
Astropower Laboratory
2121 Campus Drive
Newport Beach, California 92663
Attention: Dr. Carl Berger

Electrochimica Corporation
1140 O'Brien Drive
Menlo Park, California 94025
Attention: Dr. Morris Eisenberg

Electro-Optical Systems, Inc.
300 North Halstead Street
Pasadena, California 91107
Attention: M. Kline

Englehard Industries, Inc.
497 Delancy Street
Newark, New Jersey 07105
Attention: Dr. J. G. Cohn

Esso Research and Engineering Company
P. O. Box 8
Linden, New Jersey 07036
Attention: Dr. C. E. Heath

The Franklin Institute
Philadelphia, Pennsylvania 19105
Attention: Mr. Robert Goodman

Garrett Corporation
1625 Eye Street, N. W.
Washington, D. C. 20013
Attention: Mr. Bowler

General Dynamics/Convair
P. O. Box 1128
San Diego, California 92112
Attention: Mr. R. W. Antell
          Electrical Sys. Dept. 549-6

General Electric Company
Direct Energy Conversion Operations
Lynn, Massachusetts 01901
Attention: Dr. H. Maget

General Electric Company
Research Laboratory
Schenectady, New York 12301
Attention: Dr. H. Liebhafsky

General Motors Corporation
Box T
Santa Barbara, California 93102
Attention: Dr. C. R. Russell

Globe-Union, Inc.
900 East Keefe Avenue
Milwaukee, Wisconsin 53201

Hughes Research Laboratories Corp.
3011 Malibu Canyon Road
Malibu, California 90265
Attention: T. M. Hahn

Ionics, Incorporated
152 Sixth Street
Cambridge, Massachusetts 02142
Attention: Dr. Werner Glass

Institute for Defense Analyses
Research & Engineering Support Div.
400 Army Navy Drive
Arlington, Virginia 22202
Attention: Dr. George C. Szego
          Dr. R. Briceland

Institute of Gas Technology
State and 34th Streets
Chicago, Illinois 60616
Attention: Dr. B. S. Baker

Johns Hopkins University
Applied Physics Laboratory
8621 Georgia Avenue
Silver Spring, Maryland 20910
Attention: W. A. Tynan

Mr. J. S. Parkinson
Johns-Manville R & E Center
P. O. Box 159
Manville, New Jersey 08835

Leesona Moos Laboratories
Lake Success Park
Community Drive
Great Neck, New York 11020
Attention: Dr. A Moos

McDonnell Aircraft Corporation
Attention: Project Gemini Office
P. O. Box 516
St. Louis, Missouri 63166

Midwest Research Institute
425 Volker Boulevard
Kansas City, Missouri 64110
Attention: Dr. B. W. Beadle

Monsanto Research Corporation
Boston Laboratories
Everett, Massachusetts 02149
Attention: Dr. J. O. Smith

Monsanto Research Corporation
Dayton Laboratory
Dayton, Ohio 44221
Attention: Librarian

North American Aviation Company
S & ID Division
Downey, California 90241
Attention: Dr. James Nash

Oklahoma State University
Stillwater, Oklahoma 74075
Attention: Prof. William L. Hughes
School of Electrical Eng.

Power Information Center
University of Pennsylvania
Moore School Building
200 South 33rd Street
Philadelphia, Pennsylvania 19104

Pratt and Whitney Aircraft Division
United Aircraft Corporation
East Hartford, Connecticut 06108
Attention: Librarian

Radio Corporation of America
Astro Division
Hightstown, New Jersey 08520
Attention: Dr. Seymour Winkler

Rocketdyne
6633 Canoga Avenue
Canoga Park, California 91304
Attention: Library, Dept. 586-306

TRW Systems
One Space Park
Redondo Beach, California 90278
Attention: Dr. A. Krausz

Speer Carbon Company
Research & Development Laboratories
Packard Road at 47th Street
Niagara Falls, New York 14304

Stanford Research Institute
820 Mission Street
So. Pasadena, California 91108
Attention: Dr. Fritz Kalhammer

Texas Instruments, Inc.
13500 North Central Expressway
Dallas, Texas 75222
Attention: Dr. Issac Trachtenberg

Thiokol Chemical Corporation
Reaction Motors Division
Denville, New Jersey 07834
Attention: Dr. D. J. Mann

TRW, Inc.
23555 Euclid Avenue
Cleveland, Ohio 44117
Attention: Librarian

Tyco Laboratories, Inc,
Bear Hill
Hickory Drive
Waltham, Massachusetts 02154
Attention: W. W. Burnett

Unified Science Associates, Inc.
826 South Arroyo Parkway
Pasadena, California 91105
Attention: Dr. Sam Naiditch

Union Carbide Corporation
12900 Snow Road
Parma, Ohio 44129
Attention: Dr. George E. Evans

University of California
Space Science Laboratory
Berkely, California 94701
Attention: Prof. Charles W. Tobias

University of Pennsylvania
Electrochemistry Laboratory
Philadelphia, Pennsylvania 19104
Attention: Prof. John O'M. Bockris

University of Pennsylvania
Philadelphia, Pennsylvania 19104
Attention: Dr. Manfred Altman

The Western Company
Suite 802, RCA Building
Washington, D. C. 20006
Attention: R. T. Fiske

Western Reserve University
Cleveland, Ohio 44101
Attention: Prof. Ernest Yeager

Westinghouse Electric Corporation
Research and Development Center
Churchill Borough
Pittsburgh, Pennsylvania 15235
Attention: Dr. A. Langer

Whittaker Corporation
Power Sources Division
9601 Canoga Avenue
Chatsworth, California 91311
Attention: Dr. M. Shaw

Yardney Electric Corporation
New York, New York 10001
Attention: Dr. George Dalin

General Motors Corporation
Research Laboratories
Electrochemistry Department
12 Mile & Mound Roads
Warren, Michigan 48090
Attention: Mr. Seward Beacom

G. M. Defense Research Lab.
P. O. Box T
Santa Barbara, California 93102
Attention: Dr. Smatko

University of Toledo
Toledo, Ohio 43606
Attention: Albertine Krohn